

# ECONOMETRICA

JOURNAL OF THE ECONOMETRIC SOCIETY

*An International Society for the Advancement of Economic  
Theory in its Relation to Statistics and Mathematics*

<http://www.econometricsociety.org/>

*Econometrica*, Vol. 81, No. 1 (January, 2013), 55–111

THE LUCAS ORCHARD

IAN MARTIN

*Stanford Graduate School of Business, Stanford University, Stanford, CA 94305,  
U.S.A.*

---

The copyright to this Article is held by the Econometric Society. It may be downloaded, printed and reproduced only for educational or research purposes, including use in course packs. No downloading or copying may be done for any commercial purpose without the explicit permission of the Econometric Society. For such commercial purposes contact the Office of the Econometric Society (contact information may be found at the website <http://www.econometricsociety.org> or in the back cover of *Econometrica*). This statement must be included on all copies of this Article that are made available electronically or in any other format.

---

## THE LUCAS ORCHARD

BY IAN MARTIN<sup>1</sup>

This paper investigates the behavior of asset prices in an endowment economy in which a representative agent with power utility consumes the dividends of multiple assets. The assets are Lucas trees; a collection of Lucas trees is a Lucas orchard. The model generates return correlations that vary endogenously, spiking at times of disaster. Since disasters spread across assets, the model generates large risk premia even for assets with stable cashflows. Very small assets may comove endogenously and hence earn positive risk premia even if their cashflows are independent of the rest of the economy. I provide conditions under which the variation in a small asset's price-dividend ratio can be attributed almost entirely to variation in its risk premium.

**KEYWORDS:** Comovement, multiple assets, small assets, disasters, Lucas tree, Fourier transform, complex analysis, cumulant-generating function.

### 0. OVERVIEW

THIS PAPER INVESTIGATES the behavior of asset prices in an endowment economy in which a representative agent with power utility consumes the dividends of  $N$  assets. The assets are Lucas (1978, 1987) trees, so I call the collection of assets a Lucas orchard. Each of the  $N$  assets is assumed to have dividend growth that is independent and identically distributed (i.i.d.) over time, though potentially correlated across assets. This framework allows for the case in which dividends follow geometric Brownian motions, but also allows for jumps in dividends. Despite its simple structure, the model generates rich interactions between the prices of assets.

I highlight the important features of the model in a pair of two-tree examples. In the first, dividends follow independent geometric Brownian motions, so the intertemporal capital asset pricing model (ICAPM) of Merton (1973) and consumption-based capital asset pricing model (consumption-CAPM) of Breeden (1979) hold; here, though, price processes are not taken as given but are determined endogenously. An asset's valuation ratio depends on its dividend share of consumption: all else equal, an asset is riskier if it contributes a large proportion of consumption than if it contributes a small proportion. A shock to one asset's dividend affects the dividend shares, and hence valuation ratios, of all other assets. A small asset experiences strong positive comovement in response to good news about a large asset's dividends, and there-

<sup>1</sup>I thank Tobias Adrian, Malcolm Baker, Thomas Baranga, Robert Barro, John Cochrane, George Constantinides, Josh Coval, Emmanuel Farhi, Xavier Gabaix, Lars Hansen, Jakub Jurek, David Laibson, Robert Lucas, Greg Mankiw, Emi Nakamura, Martin Oehmke, Lubos Pástor, Roberto Rigobon, David Skeie, Jon Steinsson, Aleh Tsyvinski, Pietro Veronesi, Luis Viceira, James Vickery, and Jiang Wang for their comments. I am particularly grateful to John Campbell and Chris Rogers for their advice; and to the editor and four anonymous referees for their detailed comments.

fore has a positive beta even though its cashflows are independent of the rest of the market. With log utility the CAPM holds, so the small asset's risk premium lines up with its beta. As risk aversion increases, risk premia rise faster than linearly, the CAPM fails, and the small asset, whose valuation ratio is sensitive to market cashflow news, earns a positive alpha.

In the second example, dividends are subject to rare disasters. Now prices, interest rates, and expected returns can jump, so the ICAPM and consumption-CAPM also fail. There is an extreme form of comovement: disasters spread across assets. If a large asset experiences a disastrous cashflow shock, its price drops and the price of the other, small, asset also drops sharply. This constitutes a new channel through which disasters can contribute to high risk premia, even in assets whose own cashflows are perfectly stable.

Small assets exhibit particularly interesting behavior when the riskless rate is low. I consider, in the  $N = 2$  case, the limit in which one asset is negligibly small by comparison with the other (which represents the market). Suppose, for example, that the two assets have independent dividends. It seems plausible that a small idiosyncratic asset should earn no risk premium and that it can be valued using a Gordon growth formula, so its dividend yield should equal the riskless rate minus expected dividend growth. This intuition is correct whenever the result of the calculation is meaningful, that is, positive. But what if the riskless rate is less than the mean dividend growth of the small asset? In this *supercritical* regime, I show that the small asset has a price-consumption ratio that, as one would expect, tends to zero in the limit; it also has a dividend yield of zero in the limit, so its expected return can be attributed entirely to expected capital gains. An unexpected phenomenon emerges: despite its independent fundamentals and negligible size, the small asset comoves endogenously, and hence earns a positive, and potentially large, risk premium. Near the limit, variation in the small asset's price-dividend ratio can be attributed almost entirely to variation in its risk premium rather than to variation in the riskless rate. The small asset's log price-dividend ratio follows an approximate random walk, so its dividend growth and return are *both* approximately i.i.d.; this cannot happen in models in which log price-dividend ratios are nonconstant but stationary (Cochrane (2008)). The small asset underreacts to own-cashflow news, and comoves positively in response to the large asset's cashflow news. These results hold in *any* calibration in which the small asset is supercritical.

I next turn to an example with three i.i.d. assets,  $N = 3$  being the largest value for which behavior across the whole state space can easily be represented graphically on paper. Large assets continue to be positively correlated with other assets, and it becomes possible to ask how small assets interact with each other. Two small assets have correlated returns not because they respond positively to each other's cashflow shocks—quite the contrary—but because they both respond strongly positively to the third, large, asset's cashflow shocks. Jumps isolate patterns in correlations that are blurred together in Brownian-motion-driven models: realized correlations spike down when a small asset experiences a jump in cashflows, and spike up when a large asset experiences a

jump in cashflows. These dramatic shifts in realized correlation do not occur in examples without jumps. With more than two assets, a small asset can be either supercritical or subcritical in the same calibration, depending on the level of interest rates in different regions of the state space.

Finally, I draw a distinction between size and value effects by considering some examples with asymmetrically distributed cashflows. When value assets are modelled as having lower mean dividend growth than growth assets, I show that the model counterfactually generates a growth premium. When value assets have higher cashflow volatility, they have counterfactually high betas, and a large value asset earns a negative alpha. The qualitatively most successful example models value assets as exposed to a background risk, perhaps labor income, that is not included in the econometrician's notion of the market. Value assets then have positive CAPM alphas, and growth assets have negative CAPM alphas; and the small-value and large-growth assets have the most positive and most negative alphas, respectively.

The tractability of the framework is due in part to the use of the cumulant-generating function (CGF). Martin (2013a) expressed the riskless rate, risk premium, and consumption-wealth ratio in terms of the CGF in the case  $N = 1$ , and the expressions found there are echoed here. There are several advantages to using CGFs. Most obviously, the model allows for jumps. But CGFs also bring a perspective that clarifies some of the proofs. If we had restricted to the lognormal special case, it would have seemed natural to prove some of the main results by tedious and unenlightening algebra. Working in more generality, it becomes clear that the same results can be proved more cleanly by exploiting convexity of the CGF. (This is not to claim that no tedious algebra remains.) Finally, the CGF wraps the technological side of the model into a convenient package that simplifies what would otherwise be extremely complicated formulas.

#### *Related Literature*

Dumas (1992) considered a two-country model with shipping costs. Menzly, Santos, and Veronesi (2004) and Santos and Veronesi (2006) presented models in which the dividend shares of assets are assumed to follow mean-reverting processes. By picking convenient functional forms for these processes, closed-form pricing formulas are available, at the cost of complicated interactions between the cashflows of different assets. Pavlova and Rigobon (2007) solved an international asset pricing model, but imposed log-linear preferences so price-dividend ratios are constant. The most closely related paper is that of Cochrane, Longstaff, and Santa-Clara (2008), who solved the model with log utility, two assets, and dividends following geometric Brownian motions.

Most proofs are in the [Appendix](#), which also contains sketch proofs that provide a high-level summary of the methodology. Supplemental Material (Martin (2013b)) and *Mathematica* notebooks used in the numerical examples are available online.

## 1. SETUP

Time is continuous, and runs from 0 to infinity. There is a representative agent with power utility over consumption  $C_t$ , with relative risk aversion  $\gamma$  (a positive integer) and time preference rate  $\rho$ . There are  $N$  assets, indexed  $j = 1, \dots, N$ , that throw off random dividend streams  $D_{jt}$ . Dividends are positive, which makes it natural to work with log dividends,  $y_{jt} \equiv \log D_{jt}$ . At time 0, the dividends  $(y_{10}, \dots, y_{N0})$  of the assets are arbitrary. The vector  $\mathbf{y}_t - \mathbf{y}_0 \equiv (y_{1t} - y_{10}, \dots, y_{Nt} - y_{N0})$  is assumed to follow a Lévy process. This is the continuous-time analogue of the discrete-time assumption that dividend growth is i.i.d. To reduce the number of cases to consider, I rule out the trivial cases in which all assets have deterministic dividends, or all have perfectly correlated log dividend growth.

DEFINITION 1: The *cumulant-generating function (CGF)*  $\mathbf{c}(\boldsymbol{\theta})$  is defined for  $\boldsymbol{\theta} \in \mathbb{R}^N$  by

$$\mathbf{c}(\boldsymbol{\theta}) \equiv \log \mathbb{E} \exp \boldsymbol{\theta}'(\mathbf{y}_{t+1} - \mathbf{y}_t) = \log \mathbb{E} \left[ \left( \frac{D_{1,t+1}}{D_{1,t}} \right)^{\theta_1} \cdots \left( \frac{D_{N,t+1}}{D_{N,t}} \right)^{\theta_N} \right].$$

The CGF  $\mathbf{c}(\boldsymbol{\theta})$  encodes the cumulants of log dividend growth; it captures all relevant information about the technological side of the model. If we write  $\mathbf{0} \equiv (0, \dots, 0)'$  for the vector of zeros, then mean log dividend growth of asset  $j$  is  $\frac{\partial \mathbf{c}}{\partial \theta_j}(\mathbf{0})$ , the variance of log dividend growth of asset  $j$  is  $\frac{\partial^2 \mathbf{c}}{\partial \theta_j^2}(\mathbf{0})$ , and the covariance between the log dividend growth of assets  $j$  and  $k$  is  $\frac{\partial^2 \mathbf{c}}{\partial \theta_j \partial \theta_k}(\mathbf{0})$ . Third-order and higher partial derivatives at the origin capture higher cumulants and co-cumulants: skewness, excess kurtosis, and so on. Since Lévy processes have i.i.d. increments, we have

$$\mathbf{c}(\boldsymbol{\theta}) = \frac{1}{h} \log \mathbb{E} \exp \boldsymbol{\theta}'(\mathbf{y}_{t+h} - \mathbf{y}_t)$$

for any  $h > 0$  and  $t \geq 0$ .

In the  $N = 2$  case,  $\boldsymbol{\theta} = (\theta_1, \theta_2)'$ , I will abuse notation slightly by writing  $\mathbf{c}(\theta_1, \theta_2)$  in place of  $\mathbf{c}((\theta_1, \theta_2)')$ ; thus, for example,  $\mathbf{c}(1, 0)$  and  $\mathbf{c}(0, 1)$  are log expected gross dividend growth of assets 1 and 2, respectively.

EXAMPLE 1: If dividend growth is lognormal, that is,  $\mathbf{y}_t = \mathbf{y}_0 + \boldsymbol{\mu}t + \mathbf{A}\mathbf{Z}_t$ , where  $\boldsymbol{\mu}$  is an  $N$ -dimensional vector of drifts,  $\mathbf{A}$  an  $N \times N$  matrix of factor loadings, and  $\mathbf{Z}_t$  an  $N$ -dimensional Brownian motion, then the CGF is  $\mathbf{c}(\boldsymbol{\theta}) = \boldsymbol{\mu}'\boldsymbol{\theta} + \boldsymbol{\theta}'\boldsymbol{\Sigma}\boldsymbol{\theta}/2$ , where  $\boldsymbol{\Sigma} \equiv \mathbf{A}\mathbf{A}'$  is the covariance matrix of log dividend growth, whose elements I write as  $\sigma_{ij}$ . If the assets have independent dividend growth, then  $\boldsymbol{\Sigma}$  is a diagonal matrix, so the CGF decomposes as  $\mathbf{c}(\boldsymbol{\theta}) = \sum_{k=1}^N \mathbf{c}_k(\theta_k)$ , where  $\mathbf{c}_k(\theta_k) \equiv \mu_k \theta_k + \sigma_{kk} \theta_k^2/2$ .

EXAMPLE 2: If log dividends follow a jump-diffusion, we can write  $\mathbf{y}_t = \mathbf{y}_0 + \boldsymbol{\mu}t + \mathbf{A}\mathbf{Z}_t + \sum_{k=1}^{K(t)} \mathbf{J}^k$ , where  $K(t)$  is a Poisson process with arrival rate  $\tilde{\omega}$  that represents the number of jumps that have taken place by time  $t$ , and  $\mathbf{J}^k$  are  $N$ -dimensional random variables that are i.i.d. across  $k$ . There may be arbitrary correlations between the  $N$  elements of  $\mathbf{J}$ . (I will write  $\mathbf{J} \equiv \mathbf{J}^1$  when I discuss the distribution of these random variables.) The CGF then acquires an extra term, whose precise nature depends on the assumptions made about the jump size distribution:  $\mathbf{c}(\boldsymbol{\theta}) = \boldsymbol{\mu}'\boldsymbol{\theta} + \boldsymbol{\theta}'\boldsymbol{\Sigma}\boldsymbol{\theta}/2 + \tilde{\omega}(\mathbb{E}e^{\boldsymbol{\theta}'\mathbf{J}} - 1)$ .

EXAMPLE 2A: There is considerable flexibility in specifying the jump distribution  $\mathbf{J}$  to allow for multiple types of jump that affect different, potentially overlapping, subsets of the assets differently. Suppose, for example, that there are two assets, and let  $p_1$ ,  $p_2$ , and  $p_3$  be probabilities summing to 1. Suppose further that with probability  $p_1$ ,  $\mathbf{J}$  shocks the log dividend of asset 1 by a Normal random variable with mean  $\mu_1^{(1)}$  and variance  $\sigma_{11}^{(1)}$ ; with probability  $p_2$ ,  $\mathbf{J}$  shocks the log dividend of asset 2 by a Normal random variable with mean  $\mu_2^{(2)}$  and variance  $\sigma_{22}^{(2)}$ ; and with probability  $p_3$ ,  $\mathbf{J}$  shocks both log dividends simultaneously by a bivariate Normal random variable with mean  $(\mu_1^{(3)}, \mu_2^{(3)})'$  and covariance matrix  $\begin{pmatrix} \sigma_{11}^{(3)} & \sigma_{12}^{(3)} \\ \sigma_{12}^{(3)} & \sigma_{22}^{(3)} \end{pmatrix}$ . This is a special case of Example 2, so the CGF is

$$(1) \quad \begin{aligned} \mathbf{c}(\theta_1, \theta_2) = & \mu_1\theta_1 + \mu_2\theta_2 + \frac{1}{2}\sigma_{11}\theta_1^2 + \sigma_{12}\theta_1\theta_2 + \frac{1}{2}\sigma_{22}\theta_2^2 \\ & + \omega_1(e^{\mu_1^{(1)}\theta_1 + (1/2)\sigma_{11}^{(1)}\theta_1^2} - 1) \\ & + \omega_2(e^{\mu_2^{(2)}\theta_2 + (1/2)\sigma_{22}^{(2)}\theta_2^2} - 1) \\ & + \omega_3(e^{\mu_1^{(3)}\theta_1 + \mu_2^{(3)}\theta_2 + (1/2)\sigma_{11}^{(3)}\theta_1^2 + \sigma_{12}^{(3)}\theta_1\theta_2 + (1/2)\sigma_{22}^{(3)}\theta_2^2} - 1), \end{aligned}$$

where  $\omega_k = \tilde{\omega} p_k$  for  $k = 1, 2, 3$ .

EXAMPLE 2B: Specializing still further, suppose that the two assets are i.i.d. Independence requires that  $\sigma_{12} = \omega_3 = 0$ . Since the assets are identically distributed, we can simplify the notation by writing  $\mu_k = \mu$ ,  $\sigma_{kk} = \sigma^2$ ,  $\mu_k^{(k)} = \mu_J$ ,  $\sigma_{kk}^{(k)} = \sigma_J^2$ , and finally  $\omega_1 = \omega_2 = \omega$  for the arrival rate of each asset's jumps. The CGF is therefore given by

$$\begin{aligned} \mathbf{c}(\theta_1, \theta_2) = & \mu\theta_1 + \mu\theta_2 + \frac{1}{2}\sigma^2\theta_1^2 + \frac{1}{2}\sigma^2\theta_2^2 \\ & + \omega(e^{\mu_J\theta_1 + (1/2)\sigma_J^2\theta_1^2} - 1) + \omega(e^{\mu_J\theta_2 + (1/2)\sigma_J^2\theta_2^2} - 1). \end{aligned}$$

The corresponding CGF for  $N$  i.i.d. assets is

$$(2) \quad \mathbf{c}(\boldsymbol{\theta}) = \sum_{k=1}^N \left[ \mu \theta_k + \frac{1}{2} \sigma^2 \theta_k^2 + \omega \left( e^{\mu_j \theta_k + (1/2) \sigma_j^2 \theta_k^2} - 1 \right) \right].$$

The fact that the CGF decomposes as a sum  $\sum_k \mathbf{c}_k(\theta_k)$  reflects the independence of dividend growth across assets, as in Example 1; and the fact that the functions  $\mathbf{c}_k(\cdot)$  are identical reflects the fact that the assets are also identically distributed. I use the CGF (2) in all the numerical examples other than those in Section 3.1, so that any correlations or asymmetries that emerge do so endogenously.

I close the model by assuming that the representative investor holds the market, and that dividends are not storable, so that  $C_t = D_{1t} + \dots + D_{Nt}$ .

## 2. TWO ASSETS

As a suggestive example, consider the problem of pricing the claim to asset 1's output with log utility. The Euler equation implies that the output claim's price is

$$\begin{aligned} P_{10} &= \mathbb{E} \int_0^\infty e^{-\rho t} \left( \frac{C_t}{C_0} \right)^{-1} D_{1t} dt \\ &= (D_{10} + D_{20}) \int_0^\infty e^{-\rho t} \mathbb{E} \left( \frac{D_{1t}}{D_{1t} + D_{2t}} \right) dt, \end{aligned}$$

and unfortunately the expectation is not easy to calculate in closed form if, say, dividends follow geometric Brownian motions. Here, though, is an instructive case in which the expectation simplifies considerably. Suppose that  $D_{1t} < 1$  and  $D_{2t} \equiv 1$  at all times  $t$ , so that asset 2 is safe, but asset 1 is subject to downward jumps (potentially of random size) at random times. Then we can expand the expectation as a geometric sum:

$$\mathbb{E} \left( \frac{D_{1t}}{1 + D_{1t}} \right) = \mathbb{E} [D_{1t} - D_{1t}^2 + D_{1t}^3 - \dots] = \sum_{n=1}^{\infty} (-1)^{n+1} D_{10}^n e^{c(n,0)t}.$$

Substituting back, we find that

$$\begin{aligned} P_{10} &= (1 + D_{10}) \int_{t=0}^{\infty} e^{-\rho t} \sum_{n=1}^{\infty} (-1)^{n+1} D_{10}^n e^{c(n,0)t} \\ &= (1 + D_{10}) \sum_{n=1}^{\infty} \frac{(-1)^{n+1} D_{10}^n}{\rho - \mathbf{c}(n, 0)}. \end{aligned}$$

Defining  $s \equiv D_{10}/(D_{10} + D_{20})$  to be the share of asset 1 in total output, we have

$$(3) \quad P_{10}/D_{10} = \frac{1}{\sqrt{s(1-s)}} \sum_{n=0}^{\infty} \frac{(-1)^n \left(\frac{s}{1-s}\right)^{n+1/2}}{\rho - \mathbf{c}(n+1, 0)}.$$

This expression is easy to evaluate numerically once asset 1’s dividend process—and hence  $\mathbf{c}(\theta, 0)$ —is specified. For example, if asset 1’s log dividend is subject to downward jumps of constant size  $-b$  arriving at rate  $\omega$ , then  $\mathbf{c}(\theta, 0) = \omega(e^{-b\theta} - 1)$ , so  $\rho - \mathbf{c}(n+1, 0) \rightarrow \rho + \omega$  as  $n \rightarrow \infty$ . Meanwhile,  $s/(1-s) < 1$  so the terms in the numerator of the summand decline at geometric rate and numerical summation will converge fast.

In this special case, we can write  $D_{1t}/(1 + D_{1t})$  as a geometric sum. In the general case, the analogous move is to write the equivalent of  $D_{1t}/(1 + D_{1t})$  as a Fourier integral before computing the expectation. The gain from doing so is that, as above, it converts the otherwise intractable function inside the expectation into an expression involving products of powers of terms in  $D_{1t}$  and  $D_{2t}$  that can be conveniently expressed in terms of the CGF.

### 2.1. The General Solution

Asset prices continue to depend on the share of consumption contributed by asset 1,  $s_t = D_{1t}/(D_{1t} + D_{2t})$ , in the general case, though it is sometimes more convenient to use a state variable that is a monotonic transformation of  $s_t$ :

$$u_t = \log\left(\frac{1-s_t}{s_t}\right) = y_{2t} - y_{1t}.$$

While  $s_t$  ranges between 0 and 1,  $u_t$  takes values between  $-\infty$  and  $+\infty$ . As asset 1 becomes small,  $u_t$  tends to infinity; as asset 1 becomes large,  $u_t$  tends to minus infinity. Since  $y_{1t}$  and  $y_{2t}$  follow Lévy processes,  $u_t$  does, too. If, say, dividends follow geometric Brownian motions with equal mean log dividend growth, then  $u_t$  is a driftless Brownian motion.

The next result supplies an integral formula for the price-dividend ratio of an asset with dividend  $D_{1t}^{\alpha_1} D_{2t}^{\alpha_2}$ . By choosing the constants  $\alpha_1$  and  $\alpha_2$  appropriately, the formula can be used to price asset 1, asset 2, and a riskless perpetuity. Here and throughout the paper,  $i$  represents  $\sqrt{-1}$ . From now on I write  $u$  and  $s$ , rather than  $u_0$  and  $s_0$ , for the current value of either state variable.

PROPOSITION 1—The Pricing Formula: *The price-dividend ratio on an asset with dividend share  $s$  that pays dividend stream  $D_{\alpha,t} \equiv D_{1t}^{\alpha_1} D_{2t}^{\alpha_2}$  is*

$$(4) \quad \frac{P_{\alpha}}{D_{\alpha}}(u) = [2 \cosh(u/2)]^{\gamma} \int_{-\infty}^{\infty} \frac{e^{iuz} \mathcal{F}_{\gamma}(z)}{\rho - \mathbf{c}(\alpha_1 - \gamma/2 - iz, \alpha_2 - \gamma/2 + iz)} dz,$$

where

$$(5) \quad \mathcal{F}_\gamma(z) \equiv \frac{1}{2\pi} \cdot \frac{\Gamma(\gamma/2 + iz)\Gamma(\gamma/2 - iz)}{\Gamma(\gamma)}.$$

PROOF: The Euler equation implies that

$$\begin{aligned} P_\alpha &= \mathbb{E} \int_0^\infty e^{-\rho t} \left( \frac{C_t}{C_0} \right)^{-\gamma} D_{1t}^{\alpha_1} D_{2t}^{\alpha_2} dt \\ &= (C_0)^\gamma \int_0^\infty e^{-\rho t} \mathbb{E} \left( \frac{e^{\alpha_1(y_{10} + \tilde{y}_{1t}) + \alpha_2(y_{20} + \tilde{y}_{2t})}}{[e^{y_{10} + \tilde{y}_{1t}} + e^{y_{20} + \tilde{y}_{2t}}]^\gamma} \right) dt, \end{aligned}$$

where I have defined  $\tilde{y}_{jt} \equiv y_{jt} - y_{j0}$ . It follows that

$$\frac{P_\alpha}{D_\alpha} = (e^{y_{10}} + e^{y_{20}})^\gamma \int_0^\infty e^{-\rho t} \mathbb{E} \left( \frac{e^{\alpha_1 \tilde{y}_{1t} + \alpha_2 \tilde{y}_{2t}}}{[e^{y_{10} + \tilde{y}_{1t}} + e^{y_{20} + \tilde{y}_{2t}}]^\gamma} \right) dt.$$

The expectation inside the integral is calculated, via a Fourier transform, in equation (21) of Appendix A.1. Interchanging the order of integration—since the integrand is absolutely integrable, Fubini's theorem applies—and writing  $u$  for  $y_{20} - y_{10}$ , we obtain (4):

$$\begin{aligned} \frac{P_\alpha}{D_\alpha} &= [2 \cosh(u/2)]^\gamma \\ &\quad \times \int_{z=-\infty}^\infty \int_{t=0}^\infty e^{-\rho t} e^{\mathbf{c}(\alpha_1 - \gamma/2 - iz, \alpha_2 - \gamma/2 + iz)t} \cdot e^{iuv} \mathcal{F}_\gamma(z) dt dz \\ &\stackrel{(a)}{=} [2 \cosh(u/2)]^\gamma \int_{-\infty}^\infty \frac{e^{iuz} \mathcal{F}_\gamma(z)}{\rho - \mathbf{c}(\alpha_1 - \gamma/2 - iz, \alpha_2 - \gamma/2 + iz)} dz. \end{aligned}$$

Equality (a) is valid if  $\text{Re}[\rho - \mathbf{c}(\alpha_1 - \gamma/2 - iz, \alpha_2 - \gamma/2 + iz)] > 0$  for all  $z \in \mathbb{R}$ . In Appendix A.4, I show that this inequality holds for all  $z \in \mathbb{R}$  if it holds at  $z = 0$ , that is, so long as  $\rho - \mathbf{c}(\alpha_1 - \gamma/2, \alpha_2 - \gamma/2) > 0$ . I refer to this as the finiteness condition, and assume that it holds when  $(\alpha_1, \alpha_2) = (1, 0)$  or  $(0, 1)$ . *Q.E.D.*

The function  $\mathcal{F}_\gamma(z)$  is strictly positive, symmetric about  $z = 0$ , where it attains its maximum, and decays exponentially fast toward zero as  $|z| \rightarrow \infty$ . Equation (22) of the Appendix provides an alternative representation of  $\mathcal{F}_\gamma(z)$  in terms of elementary functions, though it is less compact than (5).

The proof of Proposition 1 shows that, for  $s \in (0, 1)$ , finiteness of the prices of the two assets—and hence of expected utility—follows from the assumptions that  $\rho - \mathbf{c}(1 - \gamma/2, -\gamma/2) > 0$  and  $\rho - \mathbf{c}(-\gamma/2, 1 - \gamma/2) > 0$ . I also assume that  $\rho - \mathbf{c}(1 - \gamma, 0) > 0$  and  $\rho - \mathbf{c}(0, 1 - \gamma) > 0$ , so that aggregate wealth is finite at the limit points  $s = 0$  and  $s = 1$ . These assumptions are recorded in Table I.

TABLE I  
THE RESTRICTIONS IMPOSED ON THE MODEL

Restriction	Reason
$\rho - \mathbf{c}(1 - \gamma/2, -\gamma/2) > 0$	Finite price of asset 1
$\rho - \mathbf{c}(-\gamma/2, 1 - \gamma/2) > 0$	Finite price of asset 2
$\rho - \mathbf{c}(1 - \gamma, 0) > 0$	Finite aggregate wealth in limit $s \rightarrow 1$
$\rho - \mathbf{c}(0, 1 - \gamma) > 0$	Finite aggregate wealth in limit $s \rightarrow 0$

For many practical purposes, this is the end of the story, since the integral formula (4) is very well behaved and can be calculated numerically almost instantly. But the pen-and-paper approach can be pushed further in some cases using techniques from complex analysis. There are many good introductions to complex analysis (such as Stein and Shakarchi (2003)), so here I will simply recall some definitions. A complex-valued function  $f$  is *holomorphic* in a subset  $G$  of the complex plane if it is complex differentiable in  $G$ . If  $f$  is holomorphic in some punctured disc  $D'(a; r) \equiv \{z \in \mathbb{C} : 0 < |z - a| < r\}$ , but not at  $a$ , then  $a$  is an *isolated singularity*. In this case,  $f$  has a unique power series expansion  $f(z) = \sum_{n=-\infty}^{\infty} c_n(z - a)^n$  for  $z \in D'(a; r)$ . If there is some positive  $m$  such that  $c_{-m} \neq 0$  but  $c_k = 0$  for all  $k < -m$ , then the singularity at  $a$  is called a *pole (of order  $m$ )*. The *residue* of  $f$  at  $a$ , written  $\text{Res}\{f(z); a\}$ , is defined to be the coefficient on the term  $(z - a)^{-1}$  in the power series expansion of  $f(z)$ . (For example, the function  $7/z$  has a pole at  $z = 0$ , and its residue there is 7.) Functions that, like the integrand in (4), are holomorphic everywhere except at certain poles away from the path of integration are called *meromorphic*. The following key result provides a line of attack for the integral in (4) (and for the integrals in equations (6) and (8) below).

FACT 1—The Residue Theorem: Let  $\Omega$  denote a closed path of integration which is to be integrated around in an anticlockwise direction. If  $f$  is holomorphic inside and on  $\Omega$ , except at a finite number of poles at points  $a_1, \dots, a_m$  inside  $\Omega$ , then

$$\int_{\Omega} f(z) dz = 2\pi i \sum_{k=1}^m \text{Res}\{f(z); a_k\}.$$

It is an amazing—and powerful—fact that such an integral can be computed by analyzing the behavior of the integrand at its poles. I illustrate this procedure in Appendix A.2 by deriving (3) from the more general (4) as a roadmap for later results.

The expected return on an asset paying dividend stream  $D_{\alpha,t}$  can be expressed in terms of integrals similar to those that appear in the price-dividend formula, and that are also easy to evaluate numerically. The instantaneous expected return,  $R_{\alpha}$ , is defined by  $R_{\alpha} dt \equiv \mathbb{E} dP_{\alpha}/P_{\alpha} + (D_{\alpha}/P_{\alpha}) dt$ .

PROPOSITION 2—Expected Returns: *The expected return  $R_\alpha$  is*

$$(6) \quad R_\alpha(u) = \frac{\sum_{m=0}^{\gamma} \binom{\gamma}{m} e^{-mu} \int_{-\infty}^{\infty} h(z) e^{iuz} \cdot \mathbf{c}(\mathbf{w}_m(z)) dz}{\sum_{m=0}^{\gamma} \binom{\gamma}{m} e^{-mu} \int_{-\infty}^{\infty} h(z) e^{iuz} dz} + \frac{D_\alpha}{P_\alpha}(u),$$

where  $h(z) \equiv \mathcal{F}_\gamma(z)/[\rho - \mathbf{c}(\alpha_1 - \gamma/2 - iz, \alpha_2 - \gamma/2 + iz)]$  and  $\mathbf{w}_m(z) \equiv (\alpha_1 - \gamma/2 + m - iz, \alpha_2 + \gamma/2 - m + iz)$ .

Write  $B_T$  for the time-0 price of a zero-coupon bond that pays one unit of the consumption good at time  $T$ , and define the yield to time  $T$ ,  $\mathcal{Y}(T)$ , by  $B_T = e^{-\mathcal{Y}(T) \cdot T}$ , the instantaneous riskless rate by  $R_f \equiv \lim_{T \downarrow 0} \mathcal{Y}(T)$ , and the long rate by  $\mathcal{Y}(\infty) \equiv \lim_{T \rightarrow \infty} \mathcal{Y}(T)$ . The next result expresses interest rates in terms of the state variable  $u$ ; again, the formulas are easy to evaluate numerically. The framework can generate upward- or downward-sloping yield curves and humped curves with an inverse-U shape.

PROPOSITION 3—Real Interest Rates: *The yield to time  $T$  is*

$$(7) \quad \mathcal{Y}(T) = -\frac{1}{T} \log \left\{ [2 \cosh(u/2)]^\gamma \times \int_{-\infty}^{\infty} \mathcal{F}_\gamma(z) e^{iuz} \cdot e^{-[\rho - \mathbf{c}(-\gamma/2 - iz, -\gamma/2 + iz)]T} dz \right\}.$$

*The instantaneous riskless rate is*

$$(8) \quad R_f = [2 \cosh(u/2)]^\gamma \int_{-\infty}^{\infty} \mathcal{F}_\gamma(z) e^{iuz} \cdot [\rho - \mathbf{c}(-\gamma/2 - iz, -\gamma/2 + iz)] dz.$$

*The long rate is constant, independent of the current state  $u$ , and given by*

$$(9) \quad \mathcal{Y}(\infty) = \max_{q^* \in [-\gamma/2, \gamma/2]} \rho - \mathbf{c}(-\gamma/2 + q^*, -\gamma/2 - q^*).$$

*In a symmetric calibration,  $\mathcal{Y}(\infty) = \rho - \mathbf{c}(-\gamma/2, -\gamma/2)$ .*

For comparison, in a one-tree economy with all consumption drawn from tree 1, the yield curve would be flat, with an interest rate of  $\rho - \mathbf{c}(-\gamma, 0)$ ; and if all consumption were drawn from tree 2, the interest rate would be  $\rho - \mathbf{c}(0, -\gamma)$ . Equation (9) shows that the long rate is at least as high in the two-tree economy as in either one-tree economy. The long rate is *equal* to the long rate in one of these economies if the requirement in (9) that  $q^* \in [-\gamma/2, \gamma/2]$  is binding.

In the lognormal case in which the mean log dividend growth of asset  $j$  is  $\mu_j$ , the instantaneous variance of asset  $j$ 's dividend growth is  $\sigma_{jj}$ , and

the covariance of the two assets' dividend growth is  $\sigma_{12}$ , we have  $\mathbf{c}(\theta_1, \theta_2) = \mu_1\theta_1 + \mu_2\theta_2 + \frac{1}{2}\sigma_{11}\theta_1^2 + \sigma_{12}\theta_1\theta_2 + \frac{1}{2}\sigma_{22}\theta_2^2$ . So we will have  $q^* = \gamma/2$  in equation (9) if  $\mu_1 - \gamma\sigma_{12} \leq \mu_2 - \gamma\sigma_{22}$ . This is intuitive: if asset 1's mean dividend growth  $\mu_1$  is sufficiently small, then it will be negligible in the distant future, so the long rate  $\rho - \mathbf{c}(0, -\gamma)$  is determined entirely by the characteristics of asset 2. It is possible, though, for asset 1 to influence long interest rates even if its share converges to zero over time with probability 1. Suppose that  $\sigma_{12} = 0$  and  $\mu_2 - \gamma\sigma_{22} < \mu_1 < \mu_2$ . Then, even though tree 2 dominates in the long run (because  $\mu_2 > \mu_1$ ), the long rate does not equal the rate that would prevail in a tree-2 economy (because  $\mu_1 - \gamma\sigma_{12} > \mu_2 - \gamma\sigma_{22}$ ). This is an instance of a general principle that the pricing of long-dated bonds is very sensitive to bad states of the world (Martin (2012))—here, to states in which the slow-growing tree makes a significant contribution to consumption.

### 2.1.1. The Geometric Brownian Motion Case

If dividend processes follow geometric Brownian motions, then asset prices can be expressed in terms of the hypergeometric function  $F(a, b; c; z)$ . This is defined for  $|z| < 1$  by the power series

$$(10) \quad F(a, b; c; z) = 1 + \frac{a \cdot b}{1! \cdot c} z + \frac{a(a+1) \cdot b(b+1)}{2! \cdot c(c+1)} z^2 + \frac{a(a+1)(a+2) \cdot b(b+1)(b+2)}{3! \cdot c(c+1)(c+2)} z^3 + \dots,$$

and for  $|z| \geq 1$  by analytic continuation of this series with respect to  $z$ .

PROPOSITION 4: *Suppose that log dividends satisfy  $dy_j = \mu_j dt + \sqrt{\sigma_{jj}} dz_j$ , and that the covariance of the two assets' dividend growth is  $\sigma_{12}$ . Then the price-dividend ratio of the asset with dividend stream  $D_{1t}^{\alpha_1} D_{2t}^{\alpha_2}$  is*

$$(11) \quad P/D(s) = \frac{1}{B(\lambda_1 - \lambda_2)} \left[ \frac{1}{(\gamma/2 + \lambda_1)s^\gamma} F\left(\gamma, \gamma/2 + \lambda_1; 1 + \gamma/2 + \lambda_1; \frac{s-1}{s}\right) + \frac{1}{(\gamma/2 - \lambda_2)(1-s)^\gamma} F\left(\gamma, \gamma/2 - \lambda_2; 1 + \gamma/2 - \lambda_2; \frac{s}{s-1}\right) \right],$$

where  $B \equiv \frac{1}{2}X^2$ ,  $\lambda_1 \equiv \frac{\sqrt{Y^2 + X^2 Z^2} - Y}{X^2}$ , and  $\lambda_2 \equiv -\frac{\sqrt{Y^2 + X^2 Z^2} + Y}{X^2}$ , with

$$X^2 \equiv \sigma_{11} - 2\sigma_{12} + \sigma_{22},$$

$$Y \equiv \mu_1 - \mu_2 + \alpha_1(\sigma_{11} - \sigma_{12}) - \alpha_2(\sigma_{22} - \sigma_{12}) - \frac{\gamma}{2}(\sigma_{11} - \sigma_{22}),$$

$$\begin{aligned}
Z^2 &\equiv 2(\rho - \alpha_1\mu_1 - \alpha_2\mu_2) - (\alpha_1^2\sigma_{11} + 2\alpha_1\alpha_2\sigma_{12} + \alpha_2^2\sigma_{22}) \\
&\quad + \gamma[\mu_1 + \mu_2 + \alpha_1\sigma_{11} + (\alpha_1 + \alpha_2)\sigma_{12} + \alpha_2\sigma_{22}] \\
&\quad - \frac{\gamma^2}{4}(\sigma_{11} + 2\sigma_{12} + \sigma_{22}).
\end{aligned}$$

As the notation suggests,  $X^2$  and  $Z^2$  are strictly positive.

The instantaneous riskless rate is given by

$$\begin{aligned}
(12) \quad R_f &= \rho + \gamma \left[ s \left( \mu_1 + \frac{\sigma_{11}}{2} \right) + (1-s) \left( \mu_2 + \frac{\sigma_{22}}{2} \right) \right] \\
&\quad - \frac{\gamma(\gamma+1)}{2} [s^2\sigma_{11} + 2s(1-s)\sigma_{12} + (1-s)^2\sigma_{22}].
\end{aligned}$$

In special cases in which parameters are chosen carefully, it is possible to simplify (11) even further, expressing it in terms of elementary functions; see the Supplemental Material (Martin (2013b)).

Proposition 4 can be extended to the case in which log dividends follow a jump-diffusion, so long as the only type of jumps that occur are global jumps:

**DEFINITION 2—Global Jumps:** A jump is *global* if it shocks each asset's log dividend by the same amount.

If, for example, the shock to log dividends is Normally distributed, then the CGF is given by (1) with  $\omega_1 = \omega_2 = 0$ ,  $\mu_1^{(3)} = \mu_2^{(3)}$ ,  $\sigma_{11}^{(3)} = \sigma_{22}^{(3)} = \sigma_{12}^{(3)}$ , and other parameters unrestricted.

**PROPOSITION 5:** *If all jumps are global, arriving at rate  $\omega$  with size distributed according to the random variable  $J$ , then (11) continues to hold with  $\rho$  replaced by  $\rho' \equiv \rho - \omega(\mathbb{E}e^{(1-\gamma)J} - 1)$ , and (12) continues to hold with  $\rho$  replaced by  $\rho'' \equiv \rho - \omega(\mathbb{E}e^{-\gamma J} - 1)$ .*

## 2.2. Two Examples

I now explore two numerical examples. The first is a conditionally lognormal model driven by Brownian motions, so the consumption-CAPM and ICAPM hold and familiar intuition can be brought to bear. The second illustrates the effects of jumps. In each example, I consider the largest possible range of  $\gamma \geq 1$  that is consistent with the assumptions in Table I, and adjust the time preference rate,  $\rho$ , so that the long rate always equals 7% as  $\gamma$  varies.

All figures were generated by evaluating the integral formulas of Propositions 1, 2, and 3 numerically in *Mathematica* (and using Itô's lemma to calculate second-moment quantities such as betas and return volatilities in the first example).

2.2.1. *Dividends Follow Geometric Brownian Motions*

Suppose that the two assets have dividends that follow independent geometric Brownian motions with mean log dividend growth of 2% and dividend volatility of 10%. The CGF is therefore given by (2) with  $N = 2$  assets,  $\mu = 0.02$ ,  $\sigma = 0.1$ , and  $\omega = 0$ .

Mean consumption growth does not vary with  $s$ , because both assets have the same mean dividend growth. But the standard deviation of consumption growth does vary: it is lowest “in the middle,” for  $s = 0.5$ , where there is most diversification. At the edges, where  $s$  is close to 0 or to 1, one of the two assets dominates the economy, and consumption growth is more volatile: the representative agent’s eggs are all in one technological basket. Time-varying consumption growth volatility leads to a time-varying riskless rate. Figure 1(a) plots the riskless rate against asset 1’s share of output  $s$ . Riskless rates are high for intermediate values of  $s$  because consumption volatility is low, which diminishes the motive for precautionary saving. Riskless rates also respond to changing expected consumption growth, with a sensitivity that depends on the elasticity of intertemporal substitution  $1/\gamma$ , but in the present example mean consumption growth is constant.

Figure 1(b) shows the price-dividend ratio of asset 1. When  $s$  is small, asset 1 contributes a small proportion of consumption. It therefore has little systematic risk, and hence a high valuation. As its dividend share increases, its

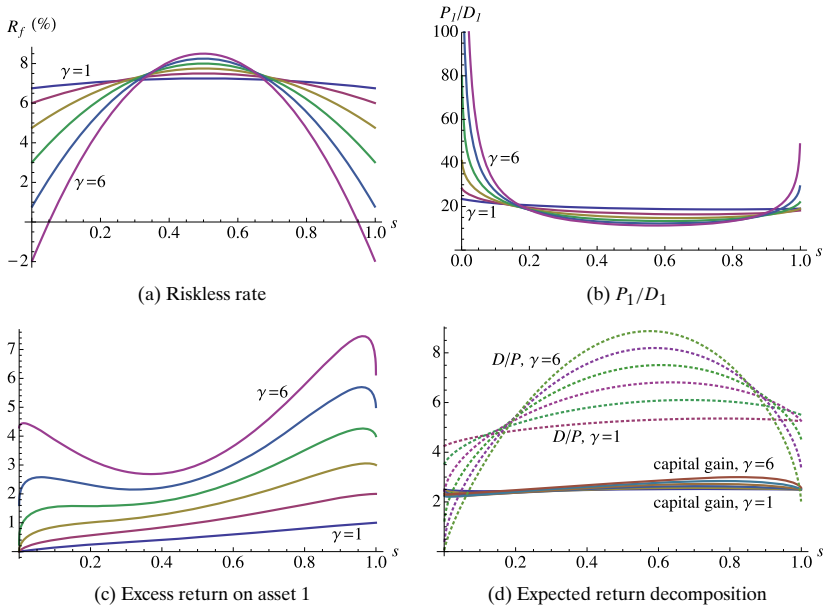


FIGURE 1.—The geometric Brownian motion example.

discount rate increases both because the riskless rate increases and because its risk premium increases, as discussed further below. The model predicts that assets may have very high price-dividend ratios but not very low price-dividend ratios. Moreover, as an asset's share approaches zero, its price-dividend ratio becomes sensitively dependent on its share.

Figure 1(c) shows the risk premium on asset 1. The consumption-CAPM holds in this calibration, so the risk premium depends on risk aversion,  $\gamma$ ; on the correlation between asset 1's return and log consumption growth,  $\kappa_{1,\Delta c}$ ; on the volatility of asset 1's return,  $\sigma_1$ ; and on the volatility of log consumption growth,  $\sigma_{\Delta c}$ . It is helpful to think of the risk premium  $= \gamma\sigma_{\Delta c}\kappa_{1,\Delta c}\sigma_1$  as the product of the price of risk,  $\gamma\sigma_{\Delta c}$ , and the quantity of risk,  $\kappa_{1,\Delta c}\sigma_1$ . The price of risk increases linearly in  $\gamma$ . For  $s$  close to zero, the quantity of risk increases in  $\gamma$ —due to an increasing correlation between asset 1's return and consumption growth, rather than to an increase in its return volatility, as we will see below—so asset 1's risk premium rises faster than linearly in  $\gamma$ . In the limit  $s \rightarrow 1$  the quantity of risk is independent of  $\gamma$ , so the risk premia march up linearly in  $\gamma$ : 1%, 2%, ..., 6%.

For fixed  $\gamma$ , asset 1's risk premium is, broadly speaking, increasing in  $s$  because larger assets have more systematic risk. The nonmonotonicity in the cases  $\gamma = 5$  and 6 reflects movements in term premia; compare with the risk premium on a perpetuity in Figure 6(a). There is a qualitative change in the risk premium of a very small asset as risk aversion increases. When  $\gamma$  equals 4, asset 1's risk premium approaches zero as  $s \rightarrow 0$ . When  $\gamma$  equals 5, asset 1 earns a positive risk premium in the limit, even though its dividends are uncorrelated with consumption growth. (This is not a term premium effect because the yield curve is flat, and perpetuities are riskless, in the limit.)

Figure 1(d) decomposes expected returns into dividend yield plus expected capital gain. Most of the time-series and cross-sectional variation in expected returns can be attributed to variation in dividend yield rather than in expected capital gains.

It might seem surprising that asset 1's risk premium achieves its maximum at a value of  $s$  close to but strictly less than 1. It does so because asset 1 has excess volatility at this point. Figure 2(a) plots the amount, in percentage points, by which asset 1's return volatility exceeds its dividend volatility. Asset 1's volatility is smaller than its dividend volatility for small  $s$  and larger for large  $s$ . Since the larger asset has a higher weight in the market, the model generates excess volatility in the aggregate market when  $\gamma > 1$  (Figure 2(b)). With log utility, there is no excess volatility because the price-dividend ratio of the aggregate market is constant. For the same reason, there is no excess volatility when  $s = 1/2$ , or equivalently,  $u = 0$ : the market price-dividend ratio is flat, as a function of  $u$ , at that point. Lastly, there is no excess volatility in the one-tree limits.

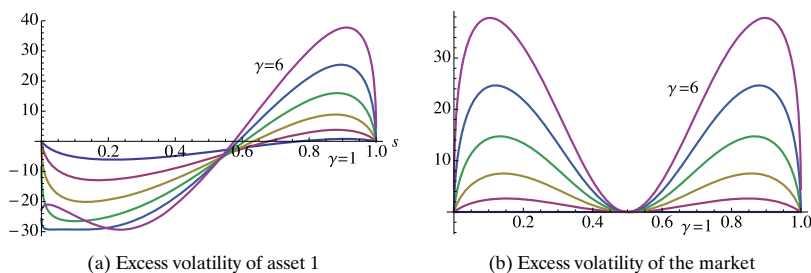


FIGURE 2.—(a) Asset 1’s excess return volatility relative to its (constant) dividend volatility. (b) The market’s excess return volatility relative to its (nonconstant) dividend volatility.

The percentage price responses of assets 1 and 2 to a 1% increase in asset 1’s dividends are shown in Figures 3(a) and 3(b). When asset 1 is small, it underreacts to a positive own-cashflow shock and asset 2 moves in the opposite direction. When asset 1 is large, it overreacts to a positive own-cashflow shock, and asset 2 comoves with it; as one would expect, cashflow shocks to a large asset have more quantitative impact than cashflow shocks to a small asset. As a result, the assets have highly correlated returns (Figure 3(c)). The amount of correlation in returns increases sharply with  $\gamma$  when one asset is significantly larger than the other. Thus the model generates, qualitatively speaking, the

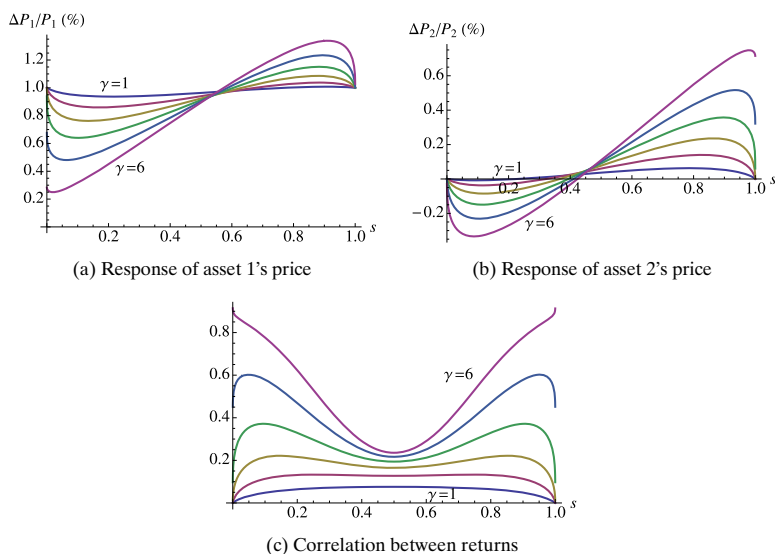


FIGURE 3.—The response of assets 1 and 2 to a 1% increase in the dividend of asset 1; and the correlation in their returns.

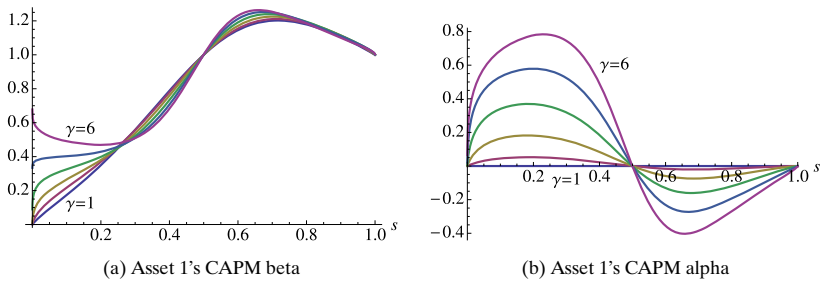


FIGURE 4.—Asset 1's CAPM alpha and beta.

“excess” comovement that is a feature of the data; Shiller (1989) showed that stock prices in the United States and United Kingdom are more correlated than cashflows, and Forbes and Rigobon (2002) found consistently high levels of interdependence between markets.

For  $\gamma$  equal to 6, asset 1's price may even react more to news about asset 2's dividend than to news about its own. To see this, observe that, for  $\gamma = 6$ , the response of asset 1's price at the left-hand side of Figure 3(a) is less than the response of asset 2's price at the right-hand side of Figure 3(b); and note that the setup is symmetrical.

Figure 4(a) plots asset 1's CAPM beta,  $\text{cov}_t(d \log P_1, d \log P_M) / \text{var}_t d \log P_M$  (where  $P_M$  is the price of the market portfolio). It is mechanically equal to 1 when  $s = 1$  (because asset 1 is the whole market) and when  $s = 1/2$  (because assets 1 and 2 are identical, and hence have identical betas, which must equal 1 because the aggregate market's beta equals 1). For the smaller values of  $\gamma$ , asset 1's beta declines toward zero as the asset's share goes to zero. But for the larger values of  $\gamma$ , asset 1 has a sizable beta even in the limit  $s \rightarrow 0$  in which its cashflows are independent of consumption growth. Figure 4(b) shows asset 1's CAPM alpha measured in percentage points. In the log utility case,  $\gamma = 1$ , the CAPM holds so its alpha is zero for all  $s$ . For larger values of  $\gamma$ , asset 1's alpha is mechanically zero at the two end points (because in a one-tree world, the market return is perfectly correlated with consumption growth, so the CAPM holds) and at  $s = 1/2$  (because the two assets are identical, so their alphas must both be zero). As asset 1's share increases from zero, its price-dividend ratio drops sharply and its alpha increases sharply. Since the aggregate market's alpha is zero, this means that the large asset must have a negative alpha.

Figure 5 plots two different decompositions of asset 1's CAPM beta. The first decomposition, which is similar to an exercise carried out by Campbell and Mei (1993), splits asset 1's return into cashflow and valuation compo-

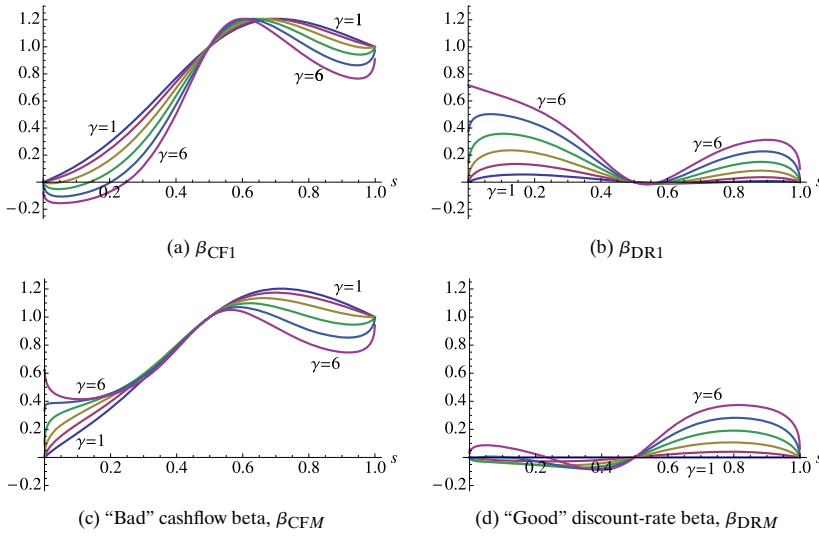


FIGURE 5.—Two decompositions of asset 1's CAPM beta.

nents:

$$\begin{aligned}
 (13) \quad & \underbrace{\frac{\text{cov}_t(d \log P_1, d \log P_M)}{\text{var}_t d \log P_M}}_{\text{CAPM beta}} \\
 &= \underbrace{\frac{\text{cov}_t(d \log D_1, d \log P_M)}{\text{var}_t d \log P_M}}_{\beta_{CF1}} + \underbrace{\frac{\text{cov}_t\left(d \log \frac{P_1}{D_1}, d \log P_M\right)}{\text{var}_t d \log P_M}}_{\beta_{DR1}}.
 \end{aligned}$$

Figures 5(a) and 5(b) show that a small asset's beta can largely be attributed to the fact that its valuation is correlated with the market return.

The second splits the *market* return into cashflow and valuation components:

$$\begin{aligned}
 (14) \quad & \underbrace{\frac{\text{cov}_t(d \log P_1, d \log P_M)}{\text{var}_t d \log P_M}}_{\text{CAPM beta}} \\
 &= \underbrace{\frac{\text{cov}_t(d \log P_1, d \log C)}{\text{var}_t d \log P_M}}_{\text{"bad" beta, } \beta_{CFM}} + \underbrace{\frac{\text{cov}_t\left(d \log P_1, d \log \frac{P_M}{C}\right)}{\text{var}_t d \log P_M}}_{\text{"good" beta, } \beta_{DRM}}.
 \end{aligned}$$

This expression breaks the CAPM beta into a “bad” cashflow beta that measures the covariance of the asset’s return with shocks to the aggregate market’s cashflows, and a “good” discount-rate beta that measures the covariance of the asset’s return with shocks to the aggregate market’s valuation ratio. It is the continuous-time version of the good-beta/bad-beta decomposition of Campbell and Vuolteenaho (2004), who derived an ICAPM result whose continuous-time analogue is that  $RP_1 = \gamma\sigma_M^2\beta_{CFM} + \sigma_M^2\beta_{DRM}$ , where  $RP_1$  denotes asset 1’s instantaneous risk premium,  $\sigma_M^2$  is the instantaneous variance of the market return, and  $\beta_{CFM}$  and  $\beta_{DRM}$  were defined in (14). The Supplemental Material (Martin (2013b)) shows that this equation holds, to a good approximation, in the present calibration. Figures 5(c) and 5(d) plot cashflow beta and discount-rate beta against  $s$ . A small asset’s CAPM beta consists almost entirely of cashflow beta. When  $\gamma = 1$ , the discount-rate beta is zero across the whole range of  $s$  because the consumption-wealth ratio, that is, the market’s valuation ratio, is constant. For larger values of  $\gamma$ , the discount-rate beta becomes a significant contributor once asset 1 is large. Since discount-rate beta earns a lower risk premium than cashflow beta, large assets earn negative alphas and small assets earn positive alphas.

To understand why the cashflow and discount-rate betas look as they do, the Supplemental Material (Martin (2013b)) carries out a further decomposition that, essentially, combines (13) and (14), splitting both asset 1’s return and the market’s return into cashflow and discount-rate components. (Campbell, Polk, and Vuolteenaho (2010) carried out this completing-the-square exercise.) The results are as suggested by Figure 5: a small asset’s beta is largely due to the high covariance of its valuation ratio with the market’s cashflows.

Figure 6(a) plots the risk premium on a perpetuity. Bonds are risky because bad times—bad news for the larger asset—are associated with the state variable moving toward  $s = 1/2$ , and hence with a rise in the riskless rate and a fall in bond prices. Figure 6(b) plots the spread between the 30-year zero-coupon yield and the instantaneous riskless rate against  $s$ . A high yield spread forecasts high excess returns on long-term bonds.

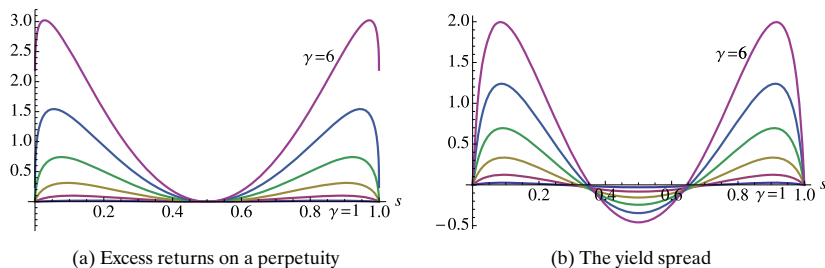


FIGURE 6.—A high yield spread signals high expected excess returns on a perpetuity.

2.2.2. Dividends Are Subject to Occasional Disasters

The second example briefly highlights the effect of disasters; it will be explored further in a three-asset example below. In addition to the two Brownian motions driving dividends, there are also jumps in dividends, representing the occurrence of disasters. Jumps arrive, independently across assets, at rate  $\omega = 0.017$ —about once every 60 years on average. When a disaster strikes an asset, it shocks its log dividend by a Normal random variable with mean  $\mu_J = -0.38$  and standard deviation  $\sigma_J = 0.25$ . These parameter values are chosen to match the disaster frequency estimated by Barro (2006) exactly, and to match the disaster size distribution documented in the same paper approximately. The CGF is as in (2) with the drifts,  $\mu$ , and the Brownian volatilities,  $\sigma$ , chosen so that the mean and variance of each asset’s log dividend growth should be the same as in the previous example. This corresponds to setting  $\mu$  and  $\sigma$  so that  $\frac{\partial c}{\partial \theta_j}(0, 0)$ , which equals mean log dividend growth of asset  $j$ , and  $\frac{\partial^2 c}{\partial \theta_j^2}(0, 0)$ , which equals the variance of log dividend growth of asset  $j$ , are as before for  $j = 1, 2$ .

Comparing Figure 7 to Figure 1, we see that, holding  $\gamma$  constant, the riskless rate is lower and the risk premium higher than in the jump-free example, for most values of  $s$ . (The highest risk aversion plotted in the figure is  $\gamma = 4$ , by comparison with  $\gamma = 6$  in the previous example.) As in Rietz (1988) and Barro (2006), incorporating rare disasters makes it easier to match observed

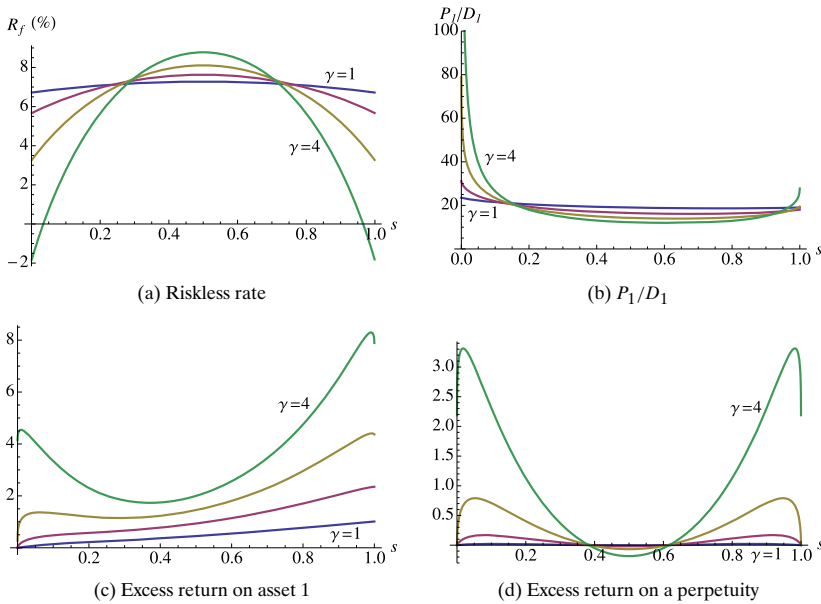


FIGURE 7.—The disaster example.

riskless rates and risk premia without requiring implausibly large  $\gamma$  (though, with power utility, disasters lead to far more variation in the riskless rate).

Disasters propagate to apparently safe assets: when the state variable jumps, interest rates and bond prices jump, too. As a result, the risk premium on a perpetuity is considerably higher than before when the current riskless rate is low, even though disasters do not affect its cashflows. The perpetuity now earns a negative risk premium at  $s = 1/2$ , even though the riskless rate is locally constant there, because it is a hedge against disasters: when a disaster strikes one of the assets, the riskless rate jumps down and the perpetuity's price jumps up.

### 2.3. *Equilibrium Behavior of a Small Asset*

A distinctive qualitative prediction of the model is that there should exist extreme growth assets, but not extreme value assets, as shown in Figure 1(b). The extreme growth case also represents the starkest departure from simple models in which price-dividend ratios are constant (as in a one-tree model with power utility and i.i.d. dividend growth). Finally, it is natural to wonder whether the complicated dynamics exhibited above are relevant for assets that are small relative to the aggregate economy. This section therefore explores the properties of asset 1 in, and near, the limit  $s \rightarrow 0$ .

Consider the problem of pricing a negligibly small asset whose cashflows are independent of consumption growth in an environment in which the riskless rate is 6%. If the small asset has mean dividend growth rate of 4%, the following logic seems plausible. Since the asset is negligibly small and idiosyncratic, it need not earn a risk premium, so the appropriate discount rate is the riskless rate. Since dividends are i.i.d., it then seems sensible to conclude from the Gordon growth model that dividend yield = riskless rate – mean dividend growth = 2%. This argument can be made formal, and I do so below. But what if the riskless rate is 2%? If the asset does not earn a risk premium, this logic seems to suggest that the dividend yield should be  $2\% - 4\% = -2\%$ , a nonsensical result.

DEFINITION 3: If the inequality

$$(15) \quad \rho - c(1, -\gamma) > 0$$

holds, we are in the *subcritical* case, while if the inequality

$$(16) \quad \rho - c(1, -\gamma) < 0$$

holds, we are in the *supercritical* case.

The quantity that appears on the left-hand side of (15) and (16) is the dividend yield on the small asset that the naive Gordon growth model logic would

predict. Consider, for example, the case in which dividend growth is independent across assets, so that the small asset's risk is idiosyncratic. Independence implies that the CGF decomposes as  $\mathbf{c}(\theta_1, \theta_2) = \mathbf{c}_1(\theta_1) + \mathbf{c}_2(\theta_2)$ , where  $\mathbf{c}_j(\theta_j) \equiv \log \mathbb{E} \exp\{\theta_j(y_{j,t+1} - y_{j,t})\}$ , so

$$\rho - \mathbf{c}(1, -\gamma) = \rho - [\mathbf{c}_1(1) + \mathbf{c}_2(-\gamma)] = \underbrace{\rho - \mathbf{c}(0, -\gamma)}_{R_f} - \underbrace{\mathbf{c}(1, 0)}_{G_1},$$

where I write  $G_1 \equiv \mathbf{c}(1, 0)$  and  $G_2 \equiv \mathbf{c}(0, 1)$  for (log) mean dividend growth on assets 1 and 2, respectively, and  $R_f$  for the limiting riskless rate, which will be shown below to equal  $\rho - \mathbf{c}(0, -\gamma)$ . More generally, if the assets are not independent, conditions (15) and (16) allow for the fact that asset 1 earns a risk premium. In the lognormal case,

$$\rho - \mathbf{c}(1, -\gamma) = R_f + \underbrace{\gamma \text{cov}(\Delta y_{1,t+1}, \Delta y_{2,t+1})}_{\text{risk premium}} - G_1.$$

Thus the subcritical case applies whenever the Gordon growth model produces a positive dividend yield; and the supercritical case applies if the Gordon growth model breaks down, predicting a negative dividend yield (as happens if  $\rho$  is sufficiently small,  $\gamma$  sufficiently large, or if cashflows are sufficiently risky so that the CGF has large curvature).

The two cases are indexed by a constant  $z^*$  that is determined by tastes,  $\rho$  and  $\gamma$ , and technologies,  $\mathbf{c}(\cdot, \cdot)$ , as the unique positive root of  $\phi(z) \equiv \rho - \mathbf{c}(1 - \gamma/2 + z, -\gamma/2 - z)$ ; thus

$$(17) \quad \rho - \mathbf{c}(1 - \gamma/2 + z^*, -\gamma/2 - z^*) = 0.$$

I show in Appendix A.6 that this equation has a unique positive solution. In the subcritical case, we have  $z^* > \gamma/2$ ; in the supercritical case, we have  $\gamma/2 - 1 < z^* < \gamma/2$ .

**PROPOSITION 6:** *In the limit as  $s \rightarrow 0$ , the Gordon growth model holds for the small asset in the subcritical case:  $D_1/P_1 = R_1 - G_1$ . Writing  $XS_i$  for the excess return on asset  $i$ , we have*

$$\begin{aligned} D_1/P_1 &= \rho - \mathbf{c}(1, -\gamma), \\ XS_1 &= \mathbf{c}(1, 0) + \mathbf{c}(0, -\gamma) - \mathbf{c}(1, -\gamma). \end{aligned}$$

*If the two assets have independent cashflows, then  $0 = XS_1 < XS_2$ .*

*In the supercritical case, the Gordon growth model fails, and we have*

$$\begin{aligned} D_1/P_1 &= 0, \\ XS_1 &= \mathbf{c}(1 - \gamma/2 + z^*, \gamma/2 - z^*) + \mathbf{c}(0, -\gamma) \\ &\quad - \mathbf{c}(1 - \gamma/2 + z^*, -\gamma/2 - z^*). \end{aligned}$$

If  $G_1 \geq G_2$ , then  $D_1/P_1 \geq R_1 - G_1$ . If the assets have independent cashflows, then  $0 < XS_1 < XS_2$ .

The Gordon growth model  $D_2/P_2 = R_2 - G_2$  holds for the large asset in both cases, and

$$R_f = \rho - \mathbf{c}(0, -\gamma),$$

$$D_2/P_2 = \rho - \mathbf{c}(0, 1 - \gamma),$$

$$XS_2 = \mathbf{c}(0, 1) + \mathbf{c}(0, -\gamma) - \mathbf{c}(0, 1 - \gamma).$$

The riskless rate and the large asset's valuation ratio and excess return are determined only by the characteristics of the large asset's dividend process, and by formulas that are exactly analogous to those derived in Martin (2013a). It is economically natural to assume, as in Table I, that the large asset's price-dividend ratio is finite in the limit, since this ensures that expected utility is finite in the limit.

But this unremarkable behavior at the macro level masks richer behavior on the part of the small asset. For there is no particular economic reason to impose the constraint that the small asset's price-dividend ratio should be finite in the limit. In the subcritical case, it will in fact be finite; then the plausible logic sketched above applies, and the small asset obeys the Gordon growth model and earns no risk premium if its cashflows are independent of the large asset's cashflows (and hence, in the limit, of consumption).

The supercritical regime is more interesting. The small asset has an enormous valuation ratio—reminiscent of Pástor and Veronesi (2003, 2006)—and one that is sensitively dependent on its dividend share.<sup>2</sup> When the large asset has bad news, the small asset's share increases and its valuation, and hence price, declines. This endogenous correlation means that the small asset earns a positive risk premium even if its cashflows are independent of consumption. Moreover, its expected return can be attributed entirely to expected capital gains because its dividend yield is zero in the limit.

Table II illustrates using the example of Section 2.2.1 with  $\gamma = 4$  (subcritical) and  $\gamma = 5$  (supercritical), and  $\rho$  adjusted so that the long rate is 7% in each case. The table holds consumption,  $D_1 + D_2$ , constant at 1, so asset 1's dividend share equals its dividend.

Near the limit, the small asset exhibits qualitatively different behavior in three different regimes. When  $z^*$ , as defined in (17), is greater than  $\gamma/2 + 1$ , the riskless rate, price-dividend ratio, and excess return of the small asset are approximately affine functions of  $s$ . The next result addresses the supercritical and *nearly supercritical* ( $z^*$  between  $\gamma/2$  and  $\gamma/2 + 1$ ) cases. The notation  $a \doteq b$  indicates that  $a$  equals  $b$  plus higher order terms in  $s$ .

<sup>2</sup>But since  $P_1/C = s \cdot P_1/D_1$ , its price-consumption ratio will tend to zero if  $P_1/D_1$  tends to infinity more slowly than  $s$  tends to zero. Appendix A.6 shows that this is indeed the case.

TABLE II  
THE SUBCRITICAL AND SUPERCRITICAL CASES<sup>a</sup>

$D_1$	$\gamma = 4$ (Subcritical, $z^* = 2.10$ )				$\gamma = 5$ (Supercritical, $z^* = 2.19$ )			
	$P_1$	$P_1/D_1$	$XS_1$	$R_f$	$P_1$	$P_1/D_1$	$XS_1$	$R_f$
0.1	2.45	24.5	1.55	4.80	2.71	<b>27.1</b>	<b>2.53</b>	3.45
0.01	0.516	51.6	1.00	3.20	0.893	<b>89.3</b>	<b>2.28</b>	1.05
0.001	0.080	79.9	0.58	3.02	0.232	<b>232</b>	<b>1.89</b>	0.78
0.0001	0.010	103.9	0.36	3.00	0.053	<b>528</b>	<b>1.70</b>	0.75
0.00001	0.001	123.3	0.24	3.00	0.011	<b>1129</b>	<b>1.61</b>	0.75
0.000001	0.000	138.8	0.17	3.00	0.002	<b>2351</b>	<b>1.58</b>	0.75
$\vdots$	$\vdots$	$\vdots$	$\vdots$	$\vdots$	$\vdots$	$\vdots$	$\vdots$	$\vdots$
0	0	200	0	3.00	0	$\infty$	<b>1.54</b>	0.75

<sup>a</sup> $D_1 + D_2$  is held constant at 1.

PROPOSITION 7: *The riskless rate is given, to leading order in  $s$ , by*

$$R_f \doteq A_1 + B_1 \cdot s.$$

*In the nearly supercritical case, the dividend yield and excess return satisfy*

$$D_1/P_1 \doteq A_2 + B_2 \cdot s^{|z^* - \gamma/2|},$$

$$XS_1 \doteq A_3 + B_3 \cdot s^{|z^* - \gamma/2|}.$$

*In the supercritical case, the dividend yield and excess return are given by*

$$D_1/P_1 \doteq B_4 \cdot s^{|z^* - \gamma/2|},$$

$$XS_1 \doteq A_5 + B_5 \cdot s^{|z^* - \gamma/2|}.$$

*The constants  $A_k$  are provided by Proposition 6 and the constants  $B_k$  are given in Appendix A.6. Dividend yields are increasing in share,  $B_2 > 0$  and  $B_4 > 0$ . If the assets have independent cashflows, then excess returns also increase in share:  $A_3 = 0$  and  $B_3 > 0$  in the nearly supercritical case, and  $A_5 > 0$  and  $B_5 > 0$  in the supercritical case.*

Since  $|z^* - \gamma/2|$  is between zero and 1,  $s^{|z^* - \gamma/2|}$  is much larger than  $s$  when  $s \approx 0$ , so the small asset's price-dividend ratio and risk premium are far more sensitive to changes in  $s$  than the riskless rate is; thus changes in its price-dividend ratio can be attributed to changes in its risk premium as opposed to changes in the interest rate.

In the supercritical case, since  $s_t \doteq e^{-u_t}$ , we have  $\log P_{1t}/D_{1t} \doteq -\log B_4 + (\gamma/2 - z^*)u_t$ . This implies that the small asset's log price-dividend ratio follows an approximate random walk. (If, say, log dividends follow Brownian motions,

then so, to first order, does  $\log P_{1t}/D_{1t}$ .) So near the limit, asset 1's one-period log return  $r_{1,t+1}$  satisfies

$$\begin{aligned}
 (18) \quad r_{1,t+1} &\doteq \Delta y_{1,t+1} + \Delta \log(P_{1,t+1}/D_{1,t+1}) \\
 &\doteq \Delta y_{1,t+1} + (\gamma/2 - z^*)\Delta u_{t+1} \\
 &= (1 - \gamma/2 + z^*)\Delta y_{1,t+1} + (\gamma/2 - z^*)\Delta y_{2,t+1}.
 \end{aligned}$$

Thus the small asset's log return and log dividend growth are *both* asymptotically i.i.d. This depends on the fact that its log price-dividend ratio follows a random walk: Cochrane (2008) showed that an asset cannot simultaneously have a time-varying price-dividend ratio, i.i.d. returns, and i.i.d. dividend growth if its log price-dividend ratio is stationary. Although stationarity may be a plausible assumption in Cochrane's application to the aggregate market, the present example shows that there is no obvious reason to assume a priori that a small asset's log price-dividend ratio is stationary.

We can rewrite (18) as a decomposition of the small asset's unexpected return into cashflow news and discount-rate news (Campbell (1991)),

$$\begin{aligned}
 r_{1,t+1} - \mathbb{E}_t r_{1,t+1} & \\
 &\doteq \underbrace{y_{1,t+1} - \mathbb{E}_t y_{1,t+1}}_{\text{cashflow news}} \\
 &\quad - \underbrace{(\gamma/2 - z^*)[(y_{1,t+1} - \mathbb{E}_t y_{1,t+1}) - (y_{2,t+1} - \mathbb{E}_t y_{2,t+1})]}_{\text{discount-rate news}}.
 \end{aligned}$$

The small asset's discount rate increases when it gets good cashflow news and declines when the large asset gets good cashflow news, *no matter what* we assume about the dividend processes of the two assets. The small asset therefore underreacts to own-cashflow news and comoves positively in response to the large asset's cashflow news.

Equation (18) has two other interesting implications. First, if  $z^*$  is sufficiently low, then the small asset's return is more sensitive to the large asset's cashflow news than it is to its own cashflow news, as in the  $\gamma = 6$  case in Figure 3. Second, since  $1 - \gamma/2 + z^*$  and  $\gamma/2 - z^*$  are positive and sum to 1, the small asset's log return is a weighted average of the two assets' log dividend growth; it follows that the small asset's return volatility cannot exceed the higher of the two cashflow volatilities. Intriguingly, Vuolteenaho (2002, Table IV) found that return volatility is indeed lower than cashflow news volatility for small stocks.

### 3. $N$ ASSETS

The basic approach is the same with  $N > 2$  assets; the main technical difficulty lies in generalizing  $\mathcal{F}_\gamma(z)$  to the  $N$ -asset case. Before stating the main

result, it will be useful to recall some old, and to define some new, notation. Let  $\mathbf{e}_j$  be the  $N$ -vector with a 1 at the  $j$ th entry and zeros elsewhere, and define the  $N$ -vectors  $\mathbf{y}_0 \equiv (y_{10}, \dots, y_{N0})'$  and  $\boldsymbol{\gamma} \equiv (\gamma, \dots, \gamma)'$ , and the  $(N - 1) \times N$  matrix  $\mathbf{U}$  and the  $(N - 1)$ -vector  $\mathbf{u} = \mathbf{U}\mathbf{y}_0$  by

$$(19) \quad \mathbf{U} \equiv \begin{pmatrix} -1 & 1 & 0 & \cdots & 0 \\ -1 & 0 & 1 & \ddots & \vdots \\ \vdots & \vdots & \ddots & \ddots & 0 \\ -1 & 0 & \cdots & 0 & 1 \end{pmatrix} \quad \text{and} \quad \mathbf{u} \equiv \begin{pmatrix} u_2 \\ u_3 \\ \vdots \\ u_N \end{pmatrix} \equiv \begin{pmatrix} y_{20} - y_{10} \\ y_{30} - y_{10} \\ \vdots \\ y_{N0} - y_{10} \end{pmatrix}.$$

We can move between the state vector  $\mathbf{u}$  and the set of dividend shares  $\{s_j\}_{j=2,\dots,N}$ , where  $s_j = D_{j0}/(D_{10} + \dots + D_{N0})$ , via the substitution  $u_j = \log(s_j/s_1)$ . The first entry of  $\mathbf{u}$  is  $u_2 = y_{20} - y_{10}$ , which corresponds to the state variable  $u$  of the two-asset case. More generally,  $u_j = y_{j0} - y_{10}$  is a measure of the size of asset  $j$  relative to asset 1. Consistent with this notation, I write  $u_1 \equiv y_{10} - y_{10} = 0$  and define the  $N$ -vector  $\mathbf{u}_+ \equiv (u_1, u_2, \dots, u_N)' = (0, u_2, \dots, u_N)'$  to make some formulas easier to typeset.

The next result generalizes earlier integral formulas to the  $N$ -asset case. The condition that ensures finiteness of the price of asset  $j$  is that  $\rho - \mathbf{c}(\mathbf{e}_j - \boldsymbol{\gamma}/N) > 0$ ; I assume that this holds for all  $j$ . All integrals are over  $\mathbb{R}^{N-1}$ .

PROPOSITION 8: *The price-dividend ratio on asset  $j$  is*

$$P_j/D_j = e^{-\boldsymbol{\gamma}'\mathbf{u}_+/N} (e^{u_1} + \dots + e^{u_N})^\gamma \int \frac{\mathcal{F}_\gamma^N(\mathbf{z}) e^{i\mathbf{u}'\mathbf{z}}}{\rho - \mathbf{c}(\mathbf{e}_j - \boldsymbol{\gamma}/N + i\mathbf{U}'\mathbf{z})} d\mathbf{z},$$

where

$$\mathcal{F}_\gamma^N(\mathbf{z}) = \frac{\Gamma(\gamma/N + iz_1 + iz_2 + \dots + iz_{N-1})}{(2\pi)^{N-1}\Gamma(\gamma)} \cdot \prod_{k=1}^{N-1} \Gamma(\gamma/N - iz_k).$$

Defining the expected return by  $\text{ER}_j dt \equiv \mathbb{E}(dP_j + D_j dt)/P_j$ , we have

$$\text{ER}_j = (1 + \Phi_j)D_j/P_j,$$

where

$$\Phi_j = \sum_{\mathbf{m}} \binom{\gamma}{\mathbf{m}} e^{(\mathbf{m} - \boldsymbol{\gamma}/N)'\mathbf{u}_+} \int \frac{\mathcal{F}_\gamma^N(\mathbf{z}) e^{i\mathbf{u}'\mathbf{z}} \mathbf{c}(\mathbf{e}_j + \mathbf{m} - \boldsymbol{\gamma}/N + i\mathbf{U}'\mathbf{z})}{\rho - \mathbf{c}(\mathbf{e}_j - \boldsymbol{\gamma}/N + i\mathbf{U}'\mathbf{z})} d\mathbf{z}.$$

The sum is over all vectors  $\mathbf{m} = (m_1, \dots, m_N)'$  whose entries are nonnegative integers that add up to  $\gamma$ . I write  $\binom{\gamma}{\mathbf{m}}$  for the multinomial coefficient  $\gamma!/(m_1! \cdots m_N!)$ .

The zero-coupon yield to time  $T$  is

$$\mathcal{Y}(T) = \rho - \frac{1}{T} \log \left[ e^{-\gamma \mathbf{u}_+ / N} (e^{u_1} + \dots + e^{u_N})^\gamma \right. \\ \left. \times \int \mathcal{F}_\gamma^N(\mathbf{z}) e^{i\mathbf{u}'\mathbf{z}} e^{c(-\gamma/N + i\mathbf{U}'\mathbf{z})T} d\mathbf{z} \right].$$

The riskless rate is

$$R_f = e^{-\gamma \mathbf{u}_+ / N} (e^{u_1} + \dots + e^{u_N})^\gamma \\ \times \int \mathcal{F}_\gamma^N(\mathbf{z}) e^{i\mathbf{u}'\mathbf{z}} [\rho - c(-\gamma/N + i\mathbf{U}'\mathbf{z})] d\mathbf{z}.$$

I now evaluate these integral formulas numerically in an example with three i.i.d. trees. This is the largest  $N$  that can easily be represented graphically on the unit simplex. I set  $\gamma = 4$  and choose  $\rho$  so that the long rate is 7%; I use the same technological parameter values as in Section 2.2.2, so, relative to that section, the only change to the CGF (2) is that  $N = 3$ . The top corner represents the state  $(s_1, s_2, s_3) = (1, 0, 0)$ ; the bottom left corner represents  $(s_1, s_2, s_3) = (0, 1, 0)$ ; and the bottom right corner represents  $(s_1, s_2, s_3) = (0, 0, 1)$ . Light regions represent larger values and dark regions represent smaller values.

Figure 8(a) shows the riskless rate. The contours indicate riskless rates of 8%, 6%, ..., -2%, radiating outward from the center. The figure is symmetric

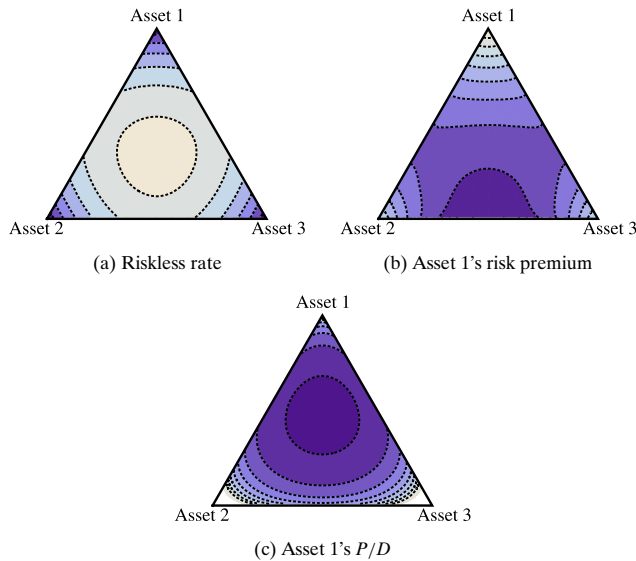


FIGURE 8.—The riskless rate, and asset 1's risk premium and price-dividend ratio.

because the calibration is symmetric. As in the two-asset case, the riskless rate is highest in the middle, where the economy is well balanced, and lowest in the corners, where one asset is dominant. Along the edges, we have copies of Figure 7(a).

Asset 1's risk premium is shown in Figure 8(b), with contours at 1%, 2%, ..., 8%, and its price-dividend ratio is shown in Figure 8(c), with contours at 14, 17, 20, ..., 35. Since the calibration is symmetric, we can also read off the excess returns and price-dividend ratios of assets 2 and 3 from the figures by relabelling appropriately. If asset 1 is dominant, it has a high risk premium and a low valuation ratio. As its share declines, its risk premium declines; this is familiar. But once asset 1 is sufficiently small, two distinct regimes emerge. In the subcritical regime in which assets 2 and 3 are of similar size, the riskless rate is relatively high, so as asset 1's share tends to zero, its valuation ratio approaches a finite limit (Figure 8(c)). In the supercritical regime, toward either of the bottom corners, where the economy is unbalanced, the riskless rate is lower than asset 1's mean dividend growth rate; as a result, asset 1's price-dividend ratio grows unboundedly and is sensitively dependent on cashflow news for the large asset, so asset 1 requires a sizable risk premium. Along the bottom edge of the simplex, asset 1's dividend yield and risk premium move in opposite directions as it shifts from one regime to the other. This phenomenon—that a small asset can be either subcritical or supercritical in the same calibration, depending on the level of interest rates—can only occur with  $N > 2$  assets.

Figure 9(a) shows how asset 1's price responds to a 1% shock to its own dividend. The contours indicate price increases of 0.5%, 0.6%, ..., 1.2%. The thick dashed contour indicates points at which the price increases by exactly 1%, that is, at which valuation ratios remain constant. When asset 1 is large—above this contour—it overreacts to own-cashflow news. When it is small, it underreacts to cashflow news, particularly in the supercritical regime in which its price-dividend ratio declines rapidly as its dividend share increases.

Figure 9(b) shows how asset 2's price responds to the 1% cashflow shock to asset 1. The contours indicate price increases of  $-0.3%$ ,  $-0.2%$ , ...,  $0.7%$ . The thick dashed contour indicates points at which asset 2's price does not respond to a cashflow shock for asset 1. If asset 1 is sufficiently large—at points above the contour—asset 2's price increases when asset 1 gets good cashflow news. If asset 1 is small, asset 2's price moves in the opposite direction following a shock to asset 1's dividend. This negative comovement is strongest toward the bottom right corner of the simplex, where asset 2 is itself small and hence in its own supercritical regime.

Figure 9(c) shows the instantaneous correlation between the returns of assets 1 and 2 due to the Brownian component of the assets' returns (i.e., conditional on no disaster arriving). The contours indicate correlations of 0% (thick dashed contour), 10%, 20%, ..., 70%. The correlation is highest of all, rising above 70%, if either asset 1 or asset 2 is dominant. It is also positive in the middle of the figure, where all three assets have the same size. This is intuitive: the

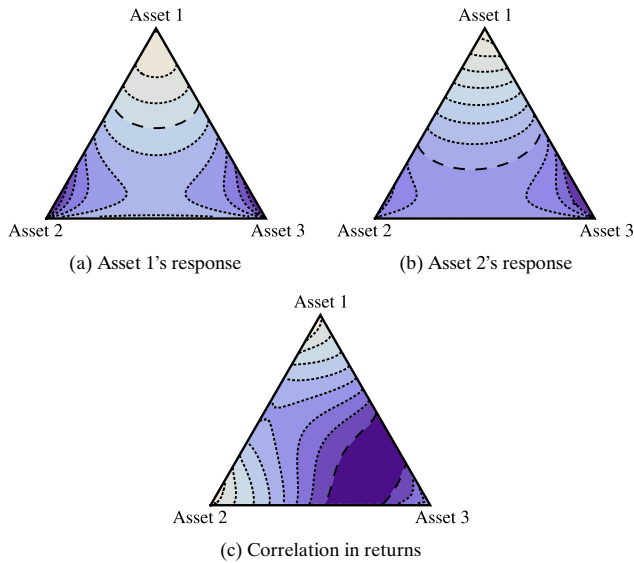


FIGURE 9.—The price response of assets 1 and 2 to a shock to asset 1's dividend, and the correlation between the returns of assets 1 and 2.

riskless rate attains its maximum at the center of the figure, so is constant near it, to first order. But cashflow shocks *do* have first order effects on risk premia in the familiar way, which induces positive comovement. The same logic applies, *mutatis mutandis*, in the middle of the left-hand edge. If both assets 1 and 2 are very small, at the bottom right of the simplex, they are positively correlated with one another. This is not because they comove in response to each other's cashflow shocks—on the contrary, they comove negatively in response to each other's shocks—but because they both comove strongly with the dominant asset 3. As asset 3 becomes less dominant, this second effect weakens, and we move into a region in which assets 1 and 2 have negatively correlated returns.

Figure 10 shows a 20-year sample path realization starting from a state of the world in which the assets have dividends of 9, 3, and 1. There are three disasters of equal severity over the sample period, one for each asset. These disasters provide a particularly clean illustration of the mechanism, since they isolate the effect of a cashflow shock to a single asset. When the small asset experiences its dividend disaster, its own price drops sharply, but the medium and large assets experience modest *upward* price jumps. When the medium asset has a disaster, the same features occur, but with more quantitative impact. When the large asset has a disaster, all the assets experience large downward price jumps.

Figure 11 plots realized return correlations over the sample path, using 1-year rolling windows. The return correlation between large and medium, and

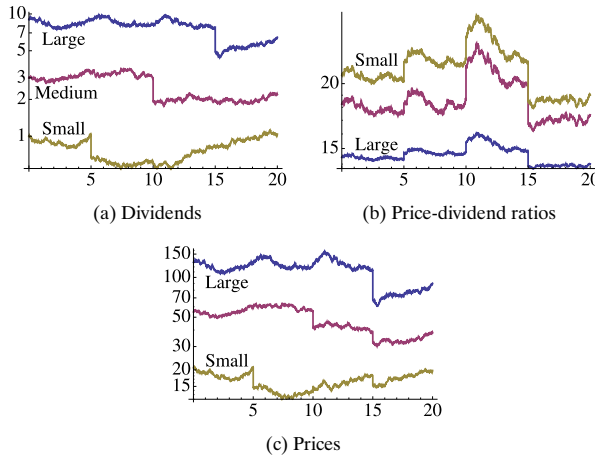


FIGURE 10.—A 20-year sample path.

between large and small, is on the order of 0.5 in normal times, as the positive comovement associated with shocks to the larger asset’s dividend outweighs the negative comovement associated with shocks to the smaller asset’s dividend. When the smaller asset experiences a disaster, however, the negative comovement comes to the fore, and we see the correlation jump down below zero. When the larger asset experiences a disaster, both the other assets move with it, and correlations spike close to 1. Finally, the correlation between the medium and small assets is close to zero in normal times due to two offsetting effects: the two assets experience negative comovement in response to each other’s cashflow shocks, but comove in response to the large asset’s shocks. The

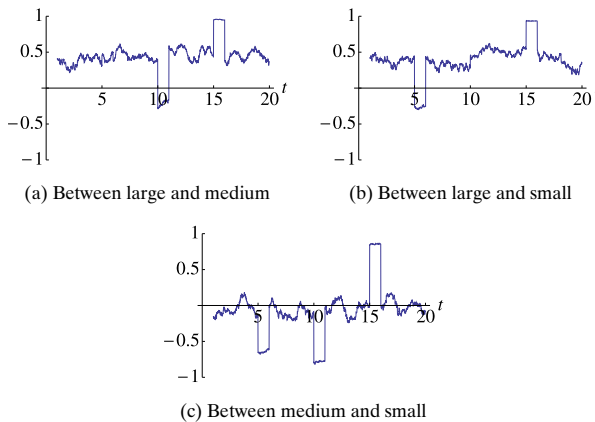


FIGURE 11.—Realized daily return correlations calculated from rolling 1-year horizons.

former effect dominates when either the small or medium asset experiences a disaster, so correlations jump below zero; and the latter effect dominates when the large asset experiences a disaster, so correlations jump up. Such spikes in return correlations are a familiar feature of the data, and here they arise in an example in which the correlation in cashflows is constant—at zero—at all times.

### 3.1. *Size versus Value*

No distinction can be drawn between size and value effects in the  $N = 2$  case, or in examples in which assets have identically distributed cashflows. To generate variation on the value dimension that does not line up perfectly with size, I now consider some examples that break the symmetry at the level of cashflows. I set  $\gamma = 4$  and choose  $\rho$  so that the long rate is 7% in each case. I arrange things so that, in each example, assets 1 through 4 are small-growth, small-value, large-growth, and large-value, respectively. There are various ways to model what makes a value asset a value asset; the following list is far from exhaustive, but it will serve to demonstrate that the different alternatives generate very different patterns of alphas and betas across the size and value dimensions:

- (i) Value assets have lower mean dividend growth.
- (ii) Value assets have more unstable cashflows.
- (iii) Value assets are more correlated with background risk.
- (iv) Value assets are exposed to background jump risk.

As always, the goal is to explore qualitative predictions of the model, so I make no attempt to optimize over parameter choices or to combine elements of this list.

To illustrate the first possibility, I consider an example in which all four assets have independent dividend growth with volatility of 10%. Assets 1 and 2 have dividend shares  $s_1 = s_2 = 0.2$ , while assets 3 and 4 have shares  $s_3 = s_4 = 0.3$ . The value assets 2 and 4 have mean log dividend growth of 1%, while the growth assets 1 and 3 have mean log dividend growth of 3%. (CGFs for all four examples are provided in the Supplemental Material.) Figure 12(a) plots CAPM alpha against CAPM beta. There is a growth premium: value stocks have high betas and negative alphas (Santos and Veronesi (2010)). This pattern is the opposite of what is observed in recent data.

In the second example, shown in Figure 12(b), all four assets have independent dividend growth with mean log dividend growth of 2%, but the two value assets have 15% volatility while the two growth assets have 5% volatility. The calibration counterfactually generates high betas for value assets and a negative alpha for the large-value asset.

In the third example, shown in Figure 12(c), I add a fifth asset with dividend share  $s_5 = 0.67$ , in line with labor's share of income. I assume that this asset, which contributes background risk, is not a part of "the market" with respect to

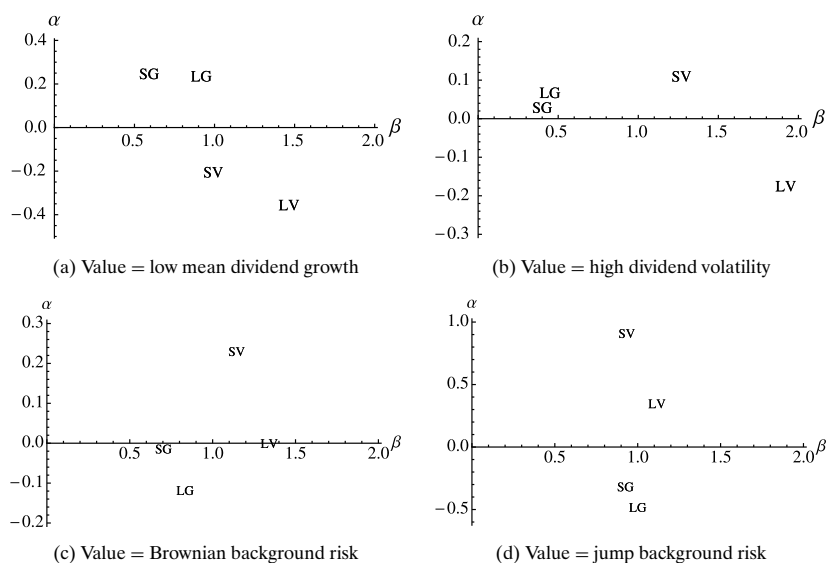


FIGURE 12.—Alphas and betas of small-growth (SG), small-value (SV), large-growth (LG), and large-value (LV) assets.

which betas are calculated. The dividend shares of the other four assets are in the same proportions as before. All five assets have mean dividend growth of 2% and dividend volatility of 10%, and the first four assets have uncorrelated cashflows; but the dividends of the two value assets have correlation of 0.5 with the fifth asset's dividend. Value assets have higher betas than growth assets. Small-growth and large-value assets have alphas close to zero, while the small-value and large-growth assets earn positive and negative alphas, respectively.

The fourth example, shown in Figure 12(d), modifies the third. Value assets now have independent Brownian motion components but experience disasters at the same time as the fifth asset. Disasters arrive at rate 0.017 and affect the value assets and the fifth asset identically. As usual, the mean log jump size is  $-0.38$  and the standard deviation is 0.25. Betas are conditional on no disaster occurring; that is, they are the betas that would be computed by an econometrician who did not observe a disaster in sample. This example comes closest to matching qualitative features of the data: betas are close to 1; value assets have positive alpha while growth assets have negative alpha; and small assets have higher alphas than large assets.

#### 4. CONCLUSION

This paper presents a frictionless multi-asset equilibrium model that generates “excess” comovement of returns relative to cashflows. Assets comove

even if their cashflows are independent, because their prices are linked via the common stochastic discount factor.

The model generalizes the work of Cochrane, Longstaff, and Santa-Clara (2008) in three directions, by allowing for power utility (rather than log), for dividends to follow exponential Lévy processes (rather than geometric Brownian motions), and for multiple assets (rather than just two). Each of these directions introduces interesting new types of behavior. Once risk aversion is higher than 1, the CAPM fails even if dividend growth is lognormal, and many of the quantities of interest increase faster than linearly in  $\gamma$ . When we allow for jumps, the ICAPM and consumption-CAPM fail, too. Disasters spread across assets, and thereby provide a new channel for high risk premia even in assets that are not themselves subject to jumps in cashflows. Jumps generate spikes in correlations in both directions, as comovement effects that blur together in Brownian-motion-driven models are isolated at the instant of a jump. With more than two assets, we can ask how small assets interact with each other, and it becomes possible to differentiate between assets on both the size and value dimension.

Many of these effects are strongest for very small assets. The limit in which one asset is negligibly small relative to another crystallizes some distinctive features of the model and is analytically tractable. I provide general conditions under which a negligibly small, idiosyncratic asset underreacts to own-cashflow news but responds sensitively to market cashflow news, and therefore requires a positive risk premium.

At the most fundamental level, it is the interaction between multiplicative features (power utility and i.i.d. log dividend growth) and additive features (consumption is the sum of dividends) that makes the model both interesting and hard to solve. These features capture a tension that is familiar to financial economists more generally: returns compound multiplicatively, while portfolio formation is additive. Using Fourier transform methods, I provide integral formulas for prices, returns, and interest rates that can be evaluated using standard numerical integration techniques. When there are two assets whose dividends follow geometric Brownian motions, or when one of the two assets is negligibly small, the integrals can be solved in closed form using techniques from complex analysis, notably the residue theorem.

The solution method is amenable to generalization in various directions. For example, Martin (2011) allowed for imperfect substitution between the goods produced by the two trees, so that intratemporal prices enter the picture, and Chen and Joslin (2012) showed how to handle the case with non-i.i.d. dividend growth. The approach can also be adapted to compute asset price behavior in an economy with two agents with differing risk aversion and one or two trees that are potentially subject to jumps, generalizing Wang (1996) and Longstaff and Wang (2012).

There are two obvious areas to work on. The riskless rate fluctuates significantly in the model. If the model could be generalized from power utility

to Epstein–Zin (1989) preferences, then this riskless rate variation could be dampened by letting the elasticity of intertemporal substitution exceed  $1/\gamma$ . An alternative view—which calls for a more ambitious extension of the model, allowing at the very least for goods to be stored over time—is that the riskless rate is stable not for reasons related to preferences, but for reasons related to technologies. In either case, it is likely that the effect of reducing riskless rate variation would be to enlarge the region in which underreaction and positive comovement take place. A second question is whether the  $N$ -asset integral formulas can be solved explicitly in special cases. It is desirable to try to do so because these formulas are subject to the curse of dimensionality, so become computationally intractable as  $N$  increases.

## APPENDIX A: THE TWO-ASSET CASE

### A.1. *The Expectation*

This section contains a calculation used in the proof of Proposition 1. The goal is to evaluate

$$\begin{aligned} E &\equiv \mathbb{E} \left( \frac{e^{\alpha_1 \tilde{y}_{1t} + \alpha_2 \tilde{y}_{2t}}}{[e^{y_{10} + \tilde{y}_{1t}} + e^{y_{20} + \tilde{y}_{2t}}]^\gamma} \right) \\ &= e^{-\gamma/2(y_{10} + y_{20})} \cdot \mathbb{E} \left( \frac{e^{(\alpha_1 - \gamma/2)\tilde{y}_{1t} + (\alpha_2 - \gamma/2)\tilde{y}_{2t}}}{[2 \cosh((y_{20} - y_{10} + \tilde{y}_{2t} - \tilde{y}_{1t})/2)]^\gamma} \right) \end{aligned}$$

for general  $\alpha_1, \alpha_2, \gamma > 0$ ; recall that  $\tilde{y}_{jt} \equiv y_{jt} - y_{j0}$ . A word or two is in order to explain why it is natural to rearrange  $E$  like this. First, with power utility, valuation ratios should be unaffected if all assets are scaled up in size proportionally, so it is natural to look for a state variable like  $y_{20} - y_{10}$ . Second, a function must decline fast toward zero as it tends to plus or minus infinity to possess a Fourier transform. Thus it is natural to reshape the term inside the expectation into an exponential term in  $\tilde{y}_{1t}$  and  $\tilde{y}_{2t}$ , which is easy to handle with the CGF, and a term  $1/[2 \cosh(u/2)]^\gamma$  that has a Fourier transform,  $\mathcal{F}_\gamma(z)$ , which satisfies

$$(20) \quad \frac{1}{[2 \cosh(u/2)]^\gamma} = \int_{-\infty}^{\infty} e^{iuz} \mathcal{F}_\gamma(z) dz.$$

We have, then,

$$\begin{aligned} (21) \quad E &= e^{-\gamma(y_{10} + y_{20})/2} \\ &\quad \times \mathbb{E} \left[ e^{(\alpha_1 - \gamma/2)\tilde{y}_{1t} + (\alpha_2 - \gamma/2)\tilde{y}_{2t}} \int_{-\infty}^{\infty} \mathcal{F}_\gamma(z) e^{iz(y_{20} - y_{10})} e^{iz(\tilde{y}_{2t} - \tilde{y}_{1t})} dz \right] \\ &= e^{-\gamma(y_{10} + y_{20})/2} \int_{-\infty}^{\infty} \mathcal{F}_\gamma(z) e^{iz(y_{20} - y_{10})} e^{c(\alpha_1 - \gamma/2 - iz, \alpha_2 - \gamma/2 + iz)t} dz. \end{aligned}$$

By the Fourier inversion theorem, equation (20) implies that

$$\begin{aligned}\mathcal{F}_\gamma(z) &= \frac{1}{2\pi} \int_{-\infty}^{\infty} \frac{e^{-iuz}}{(2 \cosh(u/2))^\gamma} du \\ &= \frac{1}{2\pi} \int_0^1 t^{\gamma/2-iz} (1-t)^{\gamma/2+iz} \frac{dt}{t(1-t)}.\end{aligned}$$

The second equality follows via the substitution  $u = \log[t/(1-t)]$ . This integral can be evaluated in terms of  $\Gamma$ -functions, giving (5); see Andrews, Askey, and Roy (1999, p. 34).

An alternative representation of  $\mathcal{F}_\gamma(z)$  will also be useful. By contour integration, one can show that  $\mathcal{F}_1(z) = \frac{1}{2} \operatorname{sech} \pi z$  and  $\mathcal{F}_2(z) = \frac{1}{2} z \operatorname{cosech} \pi z$ . From these two facts, expression (5), and the fact that  $\Gamma(x) = (x-1)\Gamma(x-1)$ , we have, for positive integer  $\gamma$ ,

$$(22) \quad \mathcal{F}_\gamma(z) = \begin{cases} \frac{z \operatorname{cosech}(\pi z)}{2(\gamma-1)!} \cdot \prod_{n=1}^{\gamma/2-1} (z^2 + n^2), & \text{for even } \gamma, \\ \frac{\operatorname{sech}(\pi z)}{2(\gamma-1)!} \cdot \prod_{n=1}^{(\gamma-1)/2} (z^2 + (n-1/2)^2), & \text{for odd } \gamma. \end{cases}$$

### A.2. Deriving (3) From (4)

This section shows how to get to (3) from the more general (4). Both equations are easy to calculate numerically in a software package such as *Mathematica*, so the purpose of the exercise is to illustrate the application of the residue theorem and to provide a roadmap for the Brownian motion case.

To streamline the discussion, I proceed heuristically, taking as given various facts that are proved for the Brownian motion case in Appendix A.5. The expression (3) is valid for  $s < 1/2$ , that is,  $u > 0$ . Setting  $\gamma = 1$  in (4), substituting  $\alpha_1 = 1, \alpha_2 = 0$  to calculate the price-dividend ratio of asset 1, and imposing the fact that  $D_{2t} \equiv 1$ , so that  $\mathbf{c}(\theta_1, \theta_2)$  is independent of  $\theta_2$  and equals, say,  $\mathbf{c}(\theta_1, 0)$ , we get

$$(23) \quad P_{10}/D_{10} = [2 \cosh(u/2)] \cdot \int_{-\infty}^{\infty} \frac{e^{iuz} \mathcal{F}_1(z)}{\rho - \mathbf{c}(1/2 - iz, 0)} dz.$$

We now proceed in a series of steps. The basic idea is to attack (23) via the residue theorem. To do so, we must integrate around a closed contour, rather than over the real axis. Loosely speaking, we want to integrate from  $-\infty$  to  $+\infty$  and then loop back along the arc of an infinitely large semicircle. More formally, we consider the limit of a sequence of integrals around increasingly large semicircles with bases lying along the real axis. Each of these integrals

can be evaluated using the residue theorem, by summing over residues inside these increasingly large semicircles. In the limit, the contribution of the integral along the semicircular arc—as opposed to the base—tends to zero. (This often happens with integrals that are amenable to this line of attack.) The upshot is that the original integral (23) equals  $2\pi i$  times the sum of *all* the residues of the integrand  $e^{iuz} \mathcal{F}_1(z)/[\rho - \mathbf{c}(1/2 - iz, 0)]$  in the upper half-plane. These residues occur at the poles of this function, that is, at the poles of  $\mathcal{F}_1(z)$  and at the zeros of  $\rho - \mathbf{c}(1/2 - iz, 0)$ .

In this example, things are particularly simple because there are no zeros of  $\rho - \mathbf{c}(1/2 - iz, 0)$  for  $z$  in the upper half-plane. (By the finiteness condition,  $\rho - \mathbf{c}(1/2, -1/2) = \rho - \mathbf{c}(1/2, 0) > 0$ . Moreover,  $\mathbf{c}(x, 0)$  is decreasing in  $x$  since  $D_{1t} < 1$ , so  $\rho - \mathbf{c}(1/2 + k, 0) > 0$  for all  $k > 0$ . It follows from Lemma 1 of Appendix A.4 that  $\text{Re}[\rho - \mathbf{c}(1/2 - iz, 0)] \geq \rho - \mathbf{c}(\text{Re}(1/2 - iz), 0) = \rho - \mathbf{c}(1/2 + \text{Im } z, 0) > 0$  for all  $z$  in the upper half-plane.) It remains to consider the poles of  $\mathcal{F}_1(z) = (1/2\pi)\Gamma(1/2 + iz)\Gamma(1/2 - iz)$ . We will need two standard properties of the  $\Gamma$ -function. First,  $\Gamma(n) = (n - 1)!$  for positive integer  $n$ . Second,  $\Gamma(z)$  has poles only at zero and at the negative real integers, and the residue at  $-n$  is  $(-1)^n/n!$ . As a result, the poles of  $e^{iuz} \mathcal{F}_1(z)/[\rho - \mathbf{c}(1/2 - iz, 0)]$  occur at  $z = (n + 1/2)i$  for  $n = 0, 1, 2, \dots$ , and the residue at  $(n + 1/2)i$  is

$$\frac{e^{-(n+1/2)u}(-1)^n\Gamma(n+1)/n!}{2\pi i \cdot [\rho - \mathbf{c}(n+1, 0)]} = \frac{(-1)^n \left(\frac{s}{1-s}\right)^{n+1/2}}{2\pi i \cdot [\rho - \mathbf{c}(n+1, 0)]}.$$

Summing over all the residues,  $n = 0, 1, \dots$ , multiplying by  $2\pi i$ , and rearranging,

$$P/D(s) = \frac{1}{\sqrt{s(1-s)}} \sum_{n=0}^{\infty} \frac{(-1)^n \left(\frac{s}{1-s}\right)^{n+1/2}}{\rho - \mathbf{c}(n+1, 0)},$$

as in equation (3). This example illustrates the more general point that residues at two types of poles contribute to the integral: (i) poles of  $\mathcal{F}_\gamma(z)$ , which are located at regularly spaced points  $(n + \gamma/2)i$ , for  $n = 0, 1, 2, \dots$ , on the imaginary axis; and (ii) poles of  $1/[\rho - \mathbf{c}(1 - \gamma/2 - iz, -\gamma/2 + iz)]$ . The Brownian motion case is tractable because  $\mathbf{c}(\theta_1, \theta_2)$  is quadratic in  $\theta_1$  and  $\theta_2$ , so the latter poles occur at zeros of the quadratic  $\rho - \mathbf{c}(1 - \gamma/2 - iz, -\gamma/2 + iz)$ , of which there is exactly one in the upper half-plane.

### A.3. Expected Returns and Interest Rates

For convenience, I write, throughout this section,

$$h(z) \equiv \frac{\mathcal{F}_\gamma(z)}{\rho - \mathbf{c}(\alpha_1 - \gamma/2 - iz, \alpha_2 - \gamma/2 + iz)}$$

and

$$\binom{n}{m} \equiv \frac{n!}{m!(n-m)!}.$$

Introducing this notation,

$$(24) \quad P_\alpha = \int_{-\infty}^{\infty} h(z) \cdot (e^{y_{10}} + e^{y_{20}})^\gamma e^{(\alpha_1 - \gamma/2 - iz)y_{10} + (\alpha_2 - \gamma/2 + iz)y_{20}} dz \\ = \sum_{m=0}^{\gamma} \binom{\gamma}{m} \int_{-\infty}^{\infty} h(z) \cdot e^{\mathbf{w}_m(z)'y} dz,$$

where  $\mathbf{w}_m(z) \equiv (\alpha_1 - \gamma/2 + m - iz, \alpha_2 + \gamma/2 - m + iz)'$ . By Proposition 8.20 of Cont and Tankov (2004), we have  $\mathbb{E}d(e^{\mathbf{w}_m(z)'y}) = e^{\mathbf{w}_m(z)'y} \mathbf{c}(\mathbf{w}_m(z)) dt$ . Using this fact,

$$\mathbb{E}(dP_\alpha) = \left\{ \sum_{m=0}^{\gamma} \binom{\gamma}{m} \int_{-\infty}^{\infty} h(z) e^{\mathbf{w}_m(z)'y} \mathbf{c}[\mathbf{w}_m(z)] dz \right\} dt.$$

Dividing by (24) and rearranging, the expected capital gain is given by the formula

$$\frac{\mathbb{E}dP_\alpha}{P_\alpha} = \frac{\sum_{m=0}^{\gamma} \binom{\gamma}{m} e^{-mu} \int_{-\infty}^{\infty} h(z) e^{iuz} \mathbf{c}(\mathbf{w}_m(z)) dz}{\sum_{m=0}^{\gamma} \binom{\gamma}{m} e^{-mu} \int_{-\infty}^{\infty} h(z) e^{iuz} dz} dt.$$

Turning to interest rates, the Euler equation implies that

$$B_T = \mathbb{E} \left[ e^{-\rho T} \left( \frac{C_T}{C_0} \right)^{-\gamma} \right] = e^{-\rho T} C_0^\gamma \mathbb{E} \left[ \frac{1}{(D_{1T} + D_{2T})^\gamma} \right].$$

Using the result of Appendix A.1, we find that

$$B_T = e^{-\rho T} [2 \cosh(u/2)]^\gamma \int_{-\infty}^{\infty} \mathcal{F}_\gamma(z) e^{iuz} \cdot e^{c(-\gamma/2 - iz, -\gamma/2 + iz)T} dz,$$

from which (7) follows, and hence also (8) by l'Hôpital's rule.

The long rate can be calculated by the method of steepest descent. The function  $\rho - \mathbf{c}(-\gamma/2 - iz, -\gamma/2 + iz)$ , considered as a function of  $z \in \mathbb{C}$ , has a stationary point on the imaginary axis. Call it  $z^* = iq^*$ , where  $q^* \in \mathbb{R}$ ; then  $q^*$  maximizes  $\rho - \mathbf{c}(-\gamma/2 + q, -\gamma/2 - q)$ . Poles of the integrand in (7) occur at the poles of  $\mathcal{F}_\gamma(z)$ , that is, at  $\pm(\gamma/2)i, \pm(\gamma/2 + 1)i$ , and so on. If

$|q^*| < \gamma/2$ , then the contour of integration in (7) (i.e., the real axis) can be deformed to pass through  $iq^*$  without crossing a pole, and therefore without altering the value of the integral, by Cauchy's theorem. It follows that  $\mathcal{Y}(\infty) = \rho - \mathbf{c}(-\gamma/2 + q^*, -\gamma/2 - q^*)$ .

If  $|q^*| \geq \gamma/2$ , then deforming the contour of integration to pass through  $iq^*$  requires a pole to be crossed, and hence a residue to be taken into account. This residue, rather than the precise location of  $iq^*$ , dictates the behavior of the long end of the yield curve. If  $q^* > \gamma/2$ , for example, the integral to be evaluated picks up an extra term proportional to  $e^{-[\rho - \mathbf{c}(0, -\gamma)]T}$ . Since  $\rho - \mathbf{c}(-\gamma/2 + q^*, -\gamma/2 - q^*)$  is larger than  $\rho - \mathbf{c}(0, -\gamma)$  by the definition of  $q^*$ , the term in  $e^{-[\rho - \mathbf{c}(-\gamma/2 + q^*, -\gamma/2 - q^*)]T}$  vanishes in the limit, and  $\mathcal{Y}(\infty) = \rho - \mathbf{c}(0, -\gamma)$ . Moreover, the concavity of  $\rho - \mathbf{c}(-\gamma/2 + q, -\gamma/2 - q)$  as a function of  $q$  implies that  $\rho - \mathbf{c}(0, -\gamma) > \rho - \mathbf{c}(-\gamma/2 + q, -\gamma/2 - q)$  for all  $q < \gamma/2$ . An almost identical argument shows that if  $q^* < -\gamma/2$ , we have  $\mathcal{Y}(\infty) = \rho - \mathbf{c}(-\gamma, 0)$ , and that in this situation  $\rho - \mathbf{c}(-\gamma, 0) > \rho - \mathbf{c}(-\gamma/2 + q, -\gamma/2 - q)$  for all  $q > -\gamma/2$ . Equation (9) follows.

#### A.4. Consequences of the Finiteness Condition

This section derives some implications of the finiteness condition  $\rho - \mathbf{c}(\alpha_1 - \gamma/2, \alpha_2 - \gamma/2) > 0$ , which is assumed to hold for the values of  $\alpha_1$  and  $\alpha_2$  provided in Table I.

LEMMA 1: *For  $z_1, z_2 \in \mathbb{C}$ , we have  $\operatorname{Re} \mathbf{c}(z_1, z_2) \leq \mathbf{c}(\operatorname{Re} z_1, \operatorname{Re} z_2)$ . The inequality is strict if  $z_1$  and  $z_2$  have nonzero imaginary parts.*

PROOF: For any  $z \in \mathbb{C}$ ,  $\operatorname{Re} \log z = \log |z|$ . It follows that  $\operatorname{Re} \mathbf{c}(z_1, z_2) = \log |\mathbb{E} e^{z_1 \tilde{y}_{11} + z_2 \tilde{y}_{21}}| \leq \log |\mathbb{E} e^{z_1 \tilde{y}_{11} + z_2 \tilde{y}_{21}}| = \log \mathbb{E} e^{\operatorname{Re} z_1 \tilde{y}_{11} + \operatorname{Re} z_2 \tilde{y}_{21}} = \mathbf{c}(\operatorname{Re} z_1, \operatorname{Re} z_2)$ . The inequality holds with equality if the argument of  $e^{z_1 \tilde{y}_{11} + z_2 \tilde{y}_{21}}$  is almost surely constant, that is, if  $\operatorname{Im}(z_1) \tilde{y}_{11} + \operatorname{Im}(z_2) \tilde{y}_{21}$  is almost surely constant. This cannot happen if  $\operatorname{Im}(z_1)$  and  $\operatorname{Im}(z_2)$  are nonzero. Q.E.D.

LEMMA 2: *For all  $z \in \mathbb{R}$ , we have  $\rho - \operatorname{Re}[\mathbf{c}(\alpha_1 - \gamma/2 - iz, \alpha_2 - \gamma/2 + iz)] > 0$ .*

PROOF: From Lemma 1,  $\operatorname{Re} \mathbf{c}(\alpha_1 - \gamma/2 - iz, \alpha_2 - \gamma/2 + iz) \leq \mathbf{c}(\alpha_1 - \gamma/2, \alpha_2 - \gamma/2)$ , so  $\rho - \operatorname{Re} \mathbf{c}(\alpha_1 - \gamma/2 - iz, \alpha_2 - \gamma/2 + iz) \geq \rho - \mathbf{c}(\alpha_1 - \gamma/2, \alpha_2 - \gamma/2) > 0$ . Q.E.D.

DEFINITION 4: Let  $f$  be a meromorphic function. A zero (or pole) of  $f$  is *minimal* if it lies in the upper half-plane and no other such zero (or pole) has smaller imaginary part.

Lemma 2 shows that  $\rho - \mathbf{c}(\alpha_1 - \gamma/2 - iz, \alpha_2 - \gamma/2 + iz)$  has no zeros on the real axis. The following property of its minimal zero will be useful in Appendix A.6.

LEMMA 3: *If there exists a minimal zero of  $\rho - \mathbf{c}(\alpha_1 - \gamma/2 - iz, \alpha_2 - \gamma/2 + iz)$ , then it is unique and lies on the imaginary axis.*

PROOF: Let  $p + qi$  be a minimal zero, and suppose (aiming for a contradiction) that  $p \neq 0$ . Lemma 1 applies with strict inequality, so  $\rho - \mathbf{c}(\alpha_1 - \gamma/2 + q, \alpha_2 - \gamma/2 - q) < 0$ . But then the finiteness condition and the intermediate value theorem imply that there exists  $q_2 \in (0, q)$  such that  $\rho - \mathbf{c}(\alpha_1 - \gamma/2 + q_2, \alpha_2 - \gamma/2 - q_2) = 0$ . If so,  $q_2i$  is a zero with  $q_2 < q$ , so  $p + qi$  is not minimal, giving the desired contradiction. *Q.E.D.*

### A.5. The Brownian Motion Case

The broad strategy for deriving the price-dividend ratio formula was laid out in Appendix A.2: the integral formula (4) is equal to the limit of a sequence of contour integrals around increasingly large semicircles in the upper half of the complex plane. By the residue theorem, this limit can be evaluated by summing all residues of the integrand in (4) in the upper half-plane. Doing so involves some tedious calculation, but we end up at (11).

Figure 13 shows one of the integrals in this sequence, for a particular calibration and  $u > 0$ . The surface shown is the real part of the integrand in (4); several poles are visible where it explodes to infinity. The dark line indicates the semicircular contour along which we integrate, whose base lies on the real axis. By the residue theorem, the integral over the contour can be evaluated by computing the residues at those poles that happen to lie inside the semicircle. As the semicircle's radius becomes larger and larger, the integral along the base approaches (4), while the integral around the semicircular arc tends to zero. Notice how the arc of the semicircle threads between the poles that form a spine running up the imaginary axis; this is always possible because the poles are evenly spaced once we get sufficiently far up the imaginary axis.

PROOF OF PROPOSITION 4: The riskless rate  $R_f$  satisfies  $R_f dt = -\mathbb{E}(dM/M)$ , where  $M_t \equiv e^{-\rho t} C_t^{-\gamma}$ ; equation (12) follows by Itô's lemma.

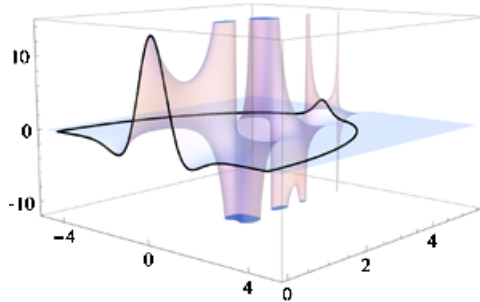


FIGURE 13.—A member of the sequence of contour integrals whose limit is (11).

In the Brownian motion case,  $\mathbf{c}(\theta_1, \theta_2) = \mu_1\theta_1 + \mu_2\theta_2 + \frac{1}{2}\sigma_{11}\theta_1^2 + \sigma_{12}\theta_1\theta_2 + \frac{1}{2}\sigma_{22}\theta_2^2$ . There are two solutions to the equation  $\rho - \mathbf{c}(\alpha_1 - \gamma/2 - iz, \alpha_2 - \gamma/2 + iz) = 0$ , each of which lies on the imaginary axis. One—call it  $\lambda_1 i$ —lies in the upper half-plane; the other—call it  $\lambda_2 i$ —lies in the lower half-plane. We can rewrite  $\rho - \mathbf{c}(\alpha_1 - \gamma/2 - iz, \alpha_2 - \gamma/2 + iz) = B(z - \lambda_1 i)(z - \lambda_2 i)$  for  $B > 0$ ,  $\lambda_1 > 0$ ,  $\lambda_2 < 0$  given in the main text. The aim, then, is to evaluate

$$(25) \quad I \equiv \int_{-\infty}^{\infty} \frac{e^{iuz} \mathcal{F}_\gamma(z)}{B(z - \lambda_1 i)(z - \lambda_2 i)} dz,$$

in terms of which the price-dividend ratio is  $P/D = [2 \cosh(u/2)]^\gamma \cdot I$ . The proof now divides into several steps. Step 1 starts from the assumption that the state variable  $u$  is positive and shows that the integral (25) can be calculated using the residue theorem. Steps 2 and 3 carry out these calculations and simplify. Step 4 extends the result to negative  $u$ .

*Step 1.* Let  $u > 0$ . Consider the case in which  $\gamma$  is even. Let  $R_n \equiv n + 1/2$ , where  $n$  is an integer. Define the large semicircle  $\Omega_n$  to be the semicircle whose base lies along the real axis from  $-R_n$  to  $R_n$  and which has a semicircular arc ( $\omega_n$ ) passing through the upper half-plane from  $R_n$  through  $R_n i$  and back to  $-R_n$ . I first show that

$$(26) \quad I = \lim_{n \rightarrow \infty} \int_{\Omega_n} \frac{e^{iuz} \mathcal{F}_\gamma(z)}{B(z - \lambda_1 i)(z - \lambda_2 i)} dz.$$

Then, from the residue theorem, it follows that

$$(27) \quad I = 2\pi i \cdot \sum \operatorname{Res} \left\{ \frac{e^{iuz} \mathcal{F}_\gamma(z)}{B(z - \lambda_1 i)(z - \lambda_2 i)}; z_p \right\},$$

where the sum is taken over all poles  $z_p$  in the upper half-plane.

The first step is to establish that (26) holds. The right-hand side is equal to

$$\lim_{n \rightarrow \infty} \underbrace{\int_{-R_n}^{R_n} \frac{e^{iuz} \mathcal{F}_\gamma(z)}{B(z - \lambda_1 i)(z - \lambda_2 i)} dz}_{I_n} + \underbrace{\int_{\omega_n} \frac{e^{iuz} \mathcal{F}_\gamma(z)}{B(z - \lambda_1 i)(z - \lambda_2 i)} dz}_{J_n}.$$

The integral  $I_n$  tends to  $I$  as  $n \rightarrow \infty$ , so the aim is to establish that the second term  $J_n$  tends to zero as  $n \rightarrow \infty$ . Along the arc  $\omega_n$ , we have  $z = R_n e^{i\theta}$ , where  $\theta$  varies between 0 and  $\pi$ . At this point, it is convenient to work with the representation of  $\mathcal{F}_\gamma(z)$  of equation (22). Substituting from (22), we have

$$J_n = \int_0^\pi \frac{e^{iuR_n \cos \theta - uR_n \sin \theta} P(R_n e^{i\theta})}{Q(R_n e^{i\theta})(e^{\pi R_n (\cos \theta + i \sin \theta)} - e^{-\pi R_n (\cos \theta + i \sin \theta)})} \cdot R_n i e^{i\theta} d\theta,$$

where  $P(\cdot)$  and  $Q(\cdot)$  are polynomials.

To show that  $J_n$  tends to zero as  $n$  tends to infinity, I separate the range of integration  $[0, \pi]$  into two parts:  $[\pi/2 - \delta, \pi/2 + \delta]$  and its complement in  $[0, \pi]$ . Here  $\delta$  will be chosen to be extremely small. First, consider

$$\begin{aligned} J_n^{(1)} &\equiv \left| \int_{\pi/2-\delta}^{\pi/2+\delta} \frac{P(R_n e^{i\theta}) e^{iuR_n \cos \theta - uR_n \sin \theta} R_n i e^{i\theta}}{Q(R_n e^{i\theta}) (e^{\pi R_n (\cos \theta + i \sin \theta)} - e^{-\pi R_n (\cos \theta + i \sin \theta)})} d\theta \right| \\ &\leq \int_{\pi/2-\delta}^{\pi/2+\delta} \left| \frac{P(R_n e^{i\theta})}{Q(R_n e^{i\theta})} \right| \frac{e^{-uR_n \sin \theta} R_n}{|e^{\pi R_n (\cos \theta + i \sin \theta)} - e^{-\pi R_n (\cos \theta + i \sin \theta)}|} d\theta. \end{aligned}$$

Pick  $\delta$  sufficiently small that

$$\left| e^{\pi R_n (\cos \theta + i \sin \theta)} - e^{-\pi R_n (\cos \theta + i \sin \theta)} \right| \geq 2 - \varepsilon$$

for all  $\theta \in [\pi/2 - \delta, \pi/2 + \delta]$ ;  $\varepsilon$  is some very small number close to but greater than zero. This is possible because the left-hand side is continuous, and equals 2 when  $\theta = \pi/2$ . Then,

$$(28) \quad J_n^{(1)} \leq \int_{\pi/2-\delta}^{\pi/2+\delta} \left| \frac{P(R_n e^{i\theta})}{Q(R_n e^{i\theta})} \right| \frac{e^{-uR_n \sin \theta} R_n}{2 - \varepsilon} d\theta.$$

Since (i) we can also ensure that  $\delta$  is small enough that  $\sin \theta \geq \varepsilon$  for  $\theta$  in the range of integration; (ii)  $|P(R_n e^{i\theta})| \leq P_2(R_n)$ , where  $P_2$  is the polynomial obtained by taking absolute values of the coefficients in  $P$ ; (iii)  $Q(R_n e^{i\theta})$  tends to infinity as  $R_n$  becomes large; and (iv) decaying exponentials decay faster than polynomials grow, in the sense that, for any positive  $k$  and  $\lambda$ ,  $x^k e^{-\lambda x} \rightarrow 0$  as  $x \rightarrow \infty$ ,  $x \in \mathbb{R}$ , we see, finally, that the right-hand side of (28), and hence  $J_n^{(1)}$ , tends to zero as  $n \rightarrow \infty$ .

It remains to be shown that

$$J_n^{(2)} \equiv \left| \int_{[0, \pi/2-\delta] \cup [\pi/2+\delta, \pi]} \frac{P(R_n e^{i\theta}) e^{iuR_n \cos \theta - uR_n \sin \theta} R_n i e^{i\theta}}{Q(R_n e^{i\theta}) (e^{\pi R_n (\cos \theta + i \sin \theta)} - e^{-\pi R_n (\cos \theta + i \sin \theta)})} d\theta \right|$$

is zero in the limit. Since  $\delta > 0$ , for all  $\theta$  in the range of integration we have that  $|\cos \theta| \geq \zeta > 0$ , for some small  $\zeta$ . We have

$$J_n^{(2)} \leq \int_{[0, \pi/2-\delta] \cup [\pi/2+\delta, \pi]} \left| \frac{P(R_n e^{i\theta})}{Q(R_n e^{i\theta})} \right| \frac{e^{-uR_n \sin \theta} R_n}{|e^{\pi R_n (\cos \theta + i \sin \theta)} - e^{-\pi R_n (\cos \theta + i \sin \theta)}|} d\theta.$$

Now,

$$\begin{aligned} \left| e^{\pi R_n (\cos \theta + i \sin \theta)} - e^{-\pi R_n (\cos \theta + i \sin \theta)} \right| &\geq \left| e^{\pi R_n (\cos \theta + i \sin \theta)} \right| - \left| e^{-\pi R_n (\cos \theta + i \sin \theta)} \right| \\ &= e^{\pi R_n |\cos \theta|} - e^{-\pi R_n |\cos \theta|} \\ &\geq e^{\pi R_n \zeta} - e^{-\pi R_n \zeta} \end{aligned}$$

for all  $\theta$  in the range of integration. So,

$$\begin{aligned} J_n^{(2)} &\leq \int_{[0, \pi/2-\delta] \cup [\pi/2+\delta, \pi]} \left| \frac{P(R_n e^{i\theta})}{Q(R_n e^{i\theta})} \right| \frac{e^{-uR_n \sin \theta} R_n}{e^{\pi R_n \zeta} - e^{-\pi R_n \zeta}} d\theta \\ &\leq \int_{[0, \pi/2-\delta] \cup [\pi/2+\delta, \pi]} \left| \frac{P(R_n e^{i\theta})}{Q(R_n e^{i\theta})} \right| \frac{R_n}{e^{\pi R_n \zeta} - e^{-\pi R_n \zeta}} d\theta, \end{aligned}$$

which tends to zero as  $n$  tends to infinity.

The case of  $\gamma$  odd is almost identical. The only important difference is that we take  $R_n = n$  (as opposed to  $n + 1/2$ ) before allowing  $n$  to go to infinity. The reason for doing so is that we must take care to avoid the poles of  $\mathcal{F}_\gamma(z)$  on the imaginary axis.

*Step 2.* From now on, I revert to the definition of  $\mathcal{F}_\gamma(z)$  given in (5). The integrand is

$$(29) \quad \frac{e^{iu z} \Gamma(\gamma/2 - iz) \Gamma(\gamma/2 + iz)}{2\pi \cdot B \cdot \Gamma(\gamma) \cdot (z - \lambda_1 i)(z - \lambda_2 i)},$$

which has poles in the upper half-plane at  $\lambda_1 i$  and at points  $z$  such that  $\gamma/2 + iz = -n$  for integers  $n \geq 0$ , since the  $\Gamma$ -function has poles at the negative integers and zero. Combining the two, (29) has poles at  $\lambda_1 i$  and at  $(n + \gamma/2)i$  for  $n \geq 0$ .

We can calculate the residue of (29) at  $z = \lambda_1 i$  directly, using the fact that if a function  $f(z) = g(z)/h(z)$  has a pole at  $a$ , and  $g(a) \neq 0$ ,  $h(a) = 0$ , and  $h'(a) \neq 0$ , then  $\text{Res}\{f(z); a\} = g(a)/h'(a)$ . The residue at  $\lambda_1 i$  is therefore

$$(30) \quad \frac{e^{-\lambda_1 u} \Gamma(\gamma/2 + \lambda_1) \Gamma(\gamma/2 - \lambda_1)}{2\pi i \cdot B \cdot \Gamma(\gamma) \cdot (\lambda_1 - \lambda_2)}.$$

For integer  $n \geq 0$ ,  $\Gamma(z)$  has residue  $(-1)^n/n!$  at  $z = -n$ , so the residue of (29) at  $(n + \gamma/2)i$  is

$$(31) \quad \frac{-e^{-u(n+\gamma/2)} \cdot \Gamma(\gamma + n) \cdot \frac{(-1)^n}{n!}}{2\pi i \cdot B \cdot \Gamma(\gamma) \cdot (n + \gamma/2 - \lambda_1)(n + \gamma/2 - \lambda_2)}.$$

Substituting (30) and (31) into (27), we find

$$\begin{aligned} I &= \frac{e^{-\lambda_1 u} \Gamma(\gamma/2 + \lambda_1) \Gamma(\gamma/2 - \lambda_1)}{B \cdot \Gamma(\gamma) \cdot (\lambda_1 - \lambda_2)} \\ &\quad - e^{-\gamma u/2} \sum_{n=0}^{\infty} \frac{(-e^{-u})^n \cdot \Gamma(\gamma + n) \cdot \frac{1}{n!}}{B \cdot \Gamma(\gamma) \cdot (n + \gamma/2 - \lambda_1)(n + \gamma/2 - \lambda_2)}. \end{aligned}$$

Since  $|-e^{-u}| < 1$  under the assumption that  $u > 0$ , which for the time being is still maintained, we can use the series definition of Gauss's hypergeometric function (10), together with the fact that  $\Gamma(\gamma + n)/\Gamma(\gamma) = \gamma(\gamma + 1) \cdots (\gamma + n - 1)$ , to obtain

$$(32) \quad I = \frac{e^{-\lambda_1 u}}{B(\lambda_1 - \lambda_2)} \frac{\Gamma(\gamma/2 - \lambda_1)\Gamma(\gamma/2 + \lambda_1)}{\Gamma(\gamma)} \\ + \frac{e^{-\gamma u/2}}{B(\lambda_1 - \lambda_2)} \left[ \frac{1}{\gamma/2 - \lambda_2} F(\gamma, \gamma/2 - \lambda_2; 1 + \gamma/2 - \lambda_2; -e^{-u}) \right. \\ \left. - \frac{1}{\gamma/2 - \lambda_1} F(\gamma, \gamma/2 - \lambda_1; 1 + \gamma/2 - \lambda_1; -e^{-u}) \right].$$

*Step 3.* A further simplification follows from the fact that

$$e^{-\lambda_1 u} \frac{\Gamma(\gamma/2 - \lambda_1)\Gamma(\gamma/2 + \lambda_1)}{\Gamma(\gamma)} \\ = \frac{e^{\gamma u/2}}{\gamma/2 + \lambda_1} F(\gamma, \gamma/2 + \lambda_1; 1 + \gamma/2 + \lambda_1; -e^{-u}) \\ + \frac{e^{-\gamma u/2}}{\gamma/2 - \lambda_1} F(\gamma, \gamma/2 - \lambda_1; 1 + \gamma/2 - \lambda_1; -e^{-u}),$$

which follows from equation (1.8.1.11) of Slater (1966, pp. 35–36). Using this in (32),

$$I = \frac{1}{B(\lambda_1 - \lambda_2)} \left[ \frac{e^{\gamma u/2}}{\gamma/2 + \lambda_1} F(\gamma, \gamma/2 + \lambda_1; 1 + \gamma/2 + \lambda_1; -e^{-u}) \right. \\ \left. + \frac{e^{-\gamma u/2}}{\gamma/2 - \lambda_2} F(\gamma, \gamma/2 - \lambda_2; 1 + \gamma/2 - \lambda_2; -e^{-u}) \right].$$

It follows that

$$(33) \quad P_1/D_1(u) \\ = \frac{[2 \cosh(u/2)]^\gamma}{B(\lambda_1 - \lambda_2)} \left[ \frac{e^{\gamma u/2}}{\gamma/2 + \lambda_1} F(\gamma, \gamma/2 + \lambda_1; 1 + \gamma/2 + \lambda_1; -e^{-u}) \right. \\ \left. + \frac{e^{-\gamma u/2}}{\gamma/2 - \lambda_2} F(\gamma, \gamma/2 - \lambda_2; 1 + \gamma/2 - \lambda_2; -e^{-u}) \right];$$

thus far, however, the derivation is valid only under the assumption that  $u > 0$ .

*Step 4.* Suppose, now, that  $u < 0$ . Take the complex conjugate of equation (25). Doing so is equivalent to reframing the problem with  $(u, \lambda_1, \lambda_2)$  replaced by  $(-u, -\lambda_2, -\lambda_1)$ . Since  $-u > 0$ ,  $-\lambda_2 > 0$ , and  $-\lambda_1 < 0$ , the method

of steps 1–4 applies unchanged. Since the formula (33) is invariant under  $(-u, -\lambda_2, -\lambda_1) \mapsto (u, \lambda_1, \lambda_2)$ , we can conclude that it is valid for all  $u$ . Substituting  $u \mapsto \log(1-s)/s$  delivers (11).

*Step 5.* Straightforward algebra gives the values of  $B$ ,  $\lambda_1$ , and  $\lambda_2$  in terms of the fundamental parameters. Since  $\mathbf{c}(\theta_1, \theta_2) = \mu_1\theta_1 + \mu_2\theta_2 + \frac{1}{2}\sigma_{11}\theta_1^2 + \sigma_{12}\theta_1\theta_2 + \frac{1}{2}\sigma_{22}\theta_2^2$ ,

$$(34) \quad \rho - \mathbf{c}(\alpha_1 - \gamma/2 - iz, \alpha_2 - \gamma/2 + iz) = \frac{1}{2}X^2z^2 + iYz + \frac{1}{2}Z^2,$$

where  $X^2$ ,  $Y$ , and  $Z^2$  are defined in the main text.  $X^2$  and  $Z^2$  are positive: the first because it is the variance of  $y_{21} - y_{11}$ , the second by setting  $v = 0$  in (34). *Q.E.D.*

**PROOF OF PROPOSITION 5:** The global jumps condition implies that the CGF takes the form  $\mathbf{c}(\boldsymbol{\theta}) = \boldsymbol{\theta}'\boldsymbol{\mu} + \boldsymbol{\theta}'\boldsymbol{\Sigma}\boldsymbol{\theta}/2 + \omega(\mathbb{E}e^{J(\theta_1+\theta_2)} - 1)$ , where  $\boldsymbol{\mu}$  is a vector of drifts and  $\boldsymbol{\Sigma}$  is the covariance matrix of the Brownian components of log dividend growth. In the case of the price-dividend ratio (4), we substitute  $\theta_1 = 1 - \gamma/2 - iz$  and  $\theta_2 = -\gamma/2 + iz$  into  $\mathbf{c}(\boldsymbol{\theta})$ ; in the case of the riskless rate (8), we substitute  $\theta_1 = -\gamma/2 - iz$  and  $\theta_2 = -\gamma/2 + iz$ . In each case, the sum  $\theta_1 + \theta_2$  is independent of  $z$ , so the jump component of the CGF,  $\omega(\mathbb{E}e^{J(\theta_1+\theta_2)} - 1)$ , is a constant independent of  $z$ . The result follows on folding this constant into  $\rho$ . *Q.E.D.*

### A.6. Small Asset Asymptotics

The basic idea is that the behavior of the integrals (4), (6), and (8) in the small-asset limit  $u \rightarrow \infty$  is determined only by the residue at the *minimal pole* whose imaginary part is closest to zero, because poles with larger imaginary parts are asymptotically irrelevant due to the  $e^{iuz}$  term. I show this by integrating around a contour that avoids all poles except for this minimal pole.

The key issue is the precise location of the minimal pole. In the case of the riskless rate, the minimal pole of the integrand in (8) is at the minimal pole of  $\mathcal{F}_\gamma(z)$ , which lies at  $(\gamma/2)i$  by standard properties of the  $\Gamma$ -function. In the case of the price-dividend ratio (4) or expected return (6), the minimal pole of the integrand could occur at  $(\gamma/2)i$ , but there is also the possibility that it occurs at the minimal zero of  $\rho - \mathbf{c}(1 - \gamma/2 - iz, -\gamma/2 + iz)$ . Lemma 3 in Appendix A.4 shows that such a minimal zero must lie on the imaginary axis, at  $z^*i$ , say, for some  $z^* > 0$  that satisfies  $\phi(z^*) = 0$  as in (17). But the finiteness conditions imply that  $\phi(0) > 0$  and  $\phi(\gamma/2 - 1) > 0$ , so because  $\phi(\cdot)$  is concave (since  $\mathbf{c}(\cdot, \cdot)$  is convex) we must, in fact, have  $z^* > \gamma/2 - 1$ . The question is whether  $z^*$ , if it exists, is larger or smaller than  $\gamma/2$ . In the subcritical case,  $z^*$  must (invoking concavity of  $\phi$  again) be greater than  $\gamma/2$  because the subcriticality condition is equivalent to  $\phi(\gamma/2) > 0$ . So the minimal pole of the integrand

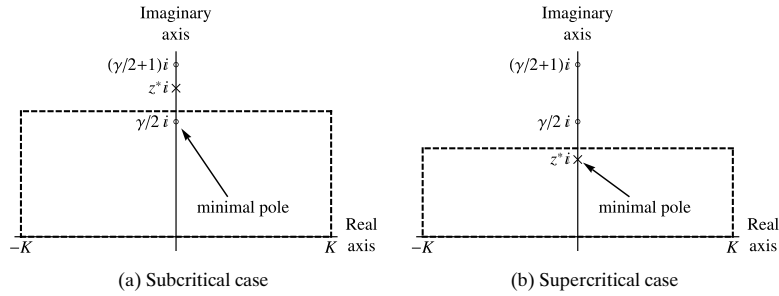


FIGURE 14.—The contour of integration in the subcritical and supercritical cases.

occurs at  $(\gamma/2)i$ , and the desired result follows on computing the residue there; this is the less interesting case. In the supercritical case,  $\phi(z)$  is now *negative* at  $z = \gamma/2$  by the supercriticality condition (16). Therefore, there is a unique  $z^* \in (\gamma/2 - 1, \gamma/2)$  solving (17), by the intermediate value theorem and concavity of  $\phi$ , and the minimal pole is at  $z^*i$ .

The two alternatives are illustrated in Figure 14, which indicates poles of  $\mathcal{F}_\gamma(z)$  with circles and marks the pole due to the zero of  $\rho - c(1 - \gamma/2 - iz, -\gamma/2 + iz)$  with a cross. (Not all poles are shown; for example,  $\mathcal{F}_\gamma(z)$  has poles at  $(\gamma/2 + m)i$  for all nonnegative integer  $m$ . There may also be other poles due to zeros of  $\rho - c(1 - \gamma/2 - iz, -\gamma/2 + iz)$ ; if so, they must lie off the imaginary axis and have imaginary parts greater than  $z^*$ .) For the sake of argument, consider the effect of increasing patience on the part of the representative agent, that is, decreasing  $\rho$ . Starting from a high value of  $\rho$ ,  $z^*$  is large (left panel). As  $\rho$  declines, the cross indicating the pole at  $z^*i$  moves smoothly down the axis. After it crosses  $(\gamma/2)i$ , it becomes the minimal pole (right panel), and there is a qualitative change in the behavior of asset 1, which becomes supercritical.

Figures 14(a) and 14(b) also show the rectangular contours around which we integrate. As  $K \rightarrow \infty$ , the integral along the base of the rectangle tends to the integral we want, and the contribution of the other three sides becomes negligible.

**PROOF OF PROPOSITION 6:** From (4), the small asset’s price-dividend ratio in the limit can be rewritten

$$(35) \quad P_1/D_1 = \lim_{u \rightarrow \infty} \frac{\int_{-\infty}^{\infty} \frac{e^{iuz} \mathcal{F}_\gamma(z)}{\rho - c(1 - \gamma/2 - iz, -\gamma/2 + iz)} dz}{\int_{-\infty}^{\infty} e^{iuz} \mathcal{F}_\gamma(z) dz}.$$

By the Riemann–Lebesgue lemma, both the numerator and denominator on the right-hand side of (35) tend to zero in the limit as  $u$  tends to infinity. What

happens to their ratio? This section shows how to calculate limiting price-dividend ratio, riskless rate, and excess returns in the small-asset case. For clarity, I work through the price-dividend ratio in detail; the same approach applies to the riskless rate and to expected returns. At the end of the section, I discuss the corresponding calculations for the large asset.

*Step 1.* Consider the integral that makes up the numerator of (35),

$$I \equiv \int_{-\infty}^{\infty} \frac{e^{iuz} \mathcal{F}_\gamma(z)}{\rho - \mathbf{c}(1 - \gamma/2 - iz, -\gamma/2 + iz)} dz.$$

If log dividends are drifting Brownian motions, Appendix A.5 showed that this integral could be approached by summing all residues in the upper half-plane. The aim here is to show that the *asymptotic* behavior of this integral in the general case is determined only by the minimal residue as discussed in the main text. To show this, I integrate around a contour that avoids all poles except for the minimal pole. Either the minimal pole occurs at the minimal zero of  $\rho - \mathbf{c}(1 - \gamma/2 - iz, -\gamma/2 + iz)$ , so lies on the imaginary axis by Lemma 3, or the minimal pole occurs at the minimal pole of  $\mathcal{F}_\gamma(z)$ , that is, at  $i\gamma/2$ . In either case, the minimal pole occurs at some point  $mi$ , where  $m > 0$  is real. See Figure 14.

Let  $\square_K$  denote the rectangle in the complex plane with corners at  $-K$ ,  $K$ ,  $K + (m + \varepsilon)i$ , and  $-K + (m + \varepsilon)i$ . Pick some tiny  $\varepsilon > 0$  such that the rectangle  $\square_K$  only contains the pole at  $mi$ . By the residue theorem, we have

$$\begin{aligned} J &\equiv \int_{\square_K} \frac{e^{iuz} \mathcal{F}_\gamma(z)}{\rho - \mathbf{c}(1 - \gamma/2 - iz, -\gamma/2 + iz)} dz \\ &= 2\pi i \operatorname{Res} \left\{ \frac{e^{iuz} \mathcal{F}_\gamma(z)}{\rho - \mathbf{c}(1 - \gamma/2 - iz, -\gamma/2 + iz)}; mi \right\}. \end{aligned}$$

To analyze this integral, we decompose it into four pieces

$$\begin{aligned} J &= \int_{-K}^K \frac{e^{iuz} \mathcal{F}_\gamma(z)}{\rho - \mathbf{c}(1 - \gamma/2 - iz, -\gamma/2 + iz)} dz \\ &\quad + \int_0^{m+\varepsilon} \frac{e^{iu(K+iz)} \mathcal{F}_\gamma(K+iz)}{\rho - \mathbf{c}(\dots)} i dz \\ &\quad + \int_K^{-K} \frac{e^{iu(z+(m+\varepsilon)i)} \mathcal{F}_\gamma(z+(m+\varepsilon)i)}{\rho - \mathbf{c}(\dots)} dz \\ &\quad + \int_{m+\varepsilon}^0 \frac{e^{iu(-K+iz)} \mathcal{F}_\gamma(-K+iz)}{\rho - \mathbf{c}(\dots)} i dz \\ &\equiv J_1 + J_2 + J_3 + J_4, \end{aligned}$$

and the goal is to show that  $J_2$ ,  $J_3$ , and  $J_4$  tend to zero as  $K$  and  $u$  tend to infinity. Consider  $J_2$ . Since the range of integration is a closed and bounded interval, the function  $|\rho - \mathbf{c}(\dots)|$  attains its maximum and minimum on the range. Since the function has no zeros on the interval, we can write  $|\rho - \mathbf{c}(\dots)| \geq \delta_1 > 0$  for all  $z$  in the range of integration. We have

$$\begin{aligned} |J_2| &\leq \int_0^{m+\varepsilon} \left| \frac{e^{iu(K+iz)} \mathcal{F}_\gamma(K+iz)}{\rho - \mathbf{c}(\dots)} i \right| dz \\ &= \int_0^{m+\varepsilon} \frac{e^{-uz} |\mathcal{F}_\gamma(K+iz)|}{|\rho - \mathbf{c}(\dots)|} dz \\ &\leq \frac{1}{\delta_1} \int_0^{m+\varepsilon} |\mathcal{F}_\gamma(K+iz)| dz \rightarrow 0 \end{aligned}$$

as  $K$  tends to infinity because  $|\mathcal{F}_\gamma(K+iz)|$  converges to zero uniformly over  $z$  in the range of integration. An almost identical argument shows that  $|J_4| \rightarrow 0$  as  $K \rightarrow \infty$ .

Now consider  $J_3$ . Set  $\delta_2 = |\rho - \mathbf{c}(1 - \gamma/2 + m + \varepsilon, -\gamma/2 - m - \varepsilon)| > 0$ . Using the results of Appendix A.4,  $|\rho - \mathbf{c}(\dots)| \geq \delta_2$  for all  $z$  in the range of integration, so

$$\begin{aligned} |J_3| &\leq \int_{-K}^K \frac{e^{-(m+\varepsilon)u} |\mathcal{F}_\gamma(z + (m+\varepsilon)i)|}{|\rho - \mathbf{c}(\dots)|} dz \\ &\leq e^{-u(m+\varepsilon)} \cdot \frac{1}{\delta_2} \int_{-K}^K |\mathcal{F}_\gamma(z + (m+\varepsilon)i)| dz \\ &\rightarrow e^{-u(m+\varepsilon)} \cdot X / \delta_2, \end{aligned}$$

where  $X = \lim_{K \rightarrow \infty} \int_{-K}^K |\mathcal{F}_\gamma(z + (m+\varepsilon)i)| dz$  is finite because  $\mathcal{F}_\gamma(z + (m+\varepsilon)i)$  decays to zero exponentially fast as  $z \rightarrow \pm\infty$ .

By the residue theorem,  $J_1 + J_2 + J_3 + J_4 = 2\pi i \times \text{residue at } mi = O(e^{-mu})$ . Now let  $K$  go to infinity.  $J_2$  and  $J_4$  tend to zero,  $J_1$  tends to  $I$ , and  $J_3$  tends to  $e^{-u(m+\varepsilon)} X$ ; so  $I + e^{-u(m+\varepsilon)} X = 2\pi i \times \text{residue at } mi = O(e^{-mu})$ .

Finally, we take the limit as  $u \rightarrow \infty$ :  $e^{-u(m+\varepsilon)} X$  is exponentially smaller than  $e^{-mu}$ , so

$I \sim 2\pi i \times \text{residue at}$

$$mi = 2\pi i \operatorname{Res} \left\{ \frac{e^{iuz} \mathcal{F}_\gamma(z)}{\rho - \mathbf{c}(1 - \gamma/2 - iz, -\gamma/2 + iz)}; mi \right\}.$$

So the asymptotic behavior of  $I$  is dictated by the residue closest to the real line.

Essentially identical arguments can be made to show that the other relevant integrals are asymptotically equivalent to  $2\pi i$  times the minimal residue of the relevant integrand.

Step 2. (i) In the price-dividend ratio case, we have to evaluate

$$(36) \quad \lim_{u \rightarrow \infty} P_1/D_1(u) = \lim_{u \rightarrow \infty} \frac{\int_{-\infty}^{\infty} \frac{e^{iuz} \mathcal{F}_\gamma(z)}{\rho - \mathbf{c}(1 - \gamma/2 - iz, -\gamma/2 + iz)} dz}{\int_{-\infty}^{\infty} e^{iuz} \mathcal{F}_\gamma(z) dz} \\ \equiv \lim_{u \rightarrow \infty} \frac{I_n}{I_d}.$$

We have seen that  $I_n$  and  $I_d$  are asymptotically equivalent to  $2\pi i$  times the residue at the pole (of the relevant integrand) with smallest imaginary part. I will refer to the pole (or zero) with least positive imaginary part as the *minimal* pole (or zero).

Consider, then, the more complicated integral  $I_n$ . The integrand has a pole at  $i\gamma/2$  due to a singularity in  $\mathcal{F}_\gamma(z)$ . The question is whether or not there is a zero of  $\rho - \mathbf{c}(1 - \gamma/2 - iz, -\gamma/2 + iz)$  for some  $z$  with imaginary part smaller than  $\gamma/2$ . If there is, then this is the minimal pole. If not, then  $i\gamma/2$  is the minimal pole. By Lemma 3, the zero in question is of the form  $z^*i$  for some positive real  $z^*$  satisfying  $\rho - \mathbf{c}(1 - \gamma/2 + z^*, -\gamma/2 - z^*) = 0$ . If  $z^* > \gamma/2$ —in the subcritical case—the minimal pole for both integrals is at  $i\gamma/2$ , so

$$P_1/D_1 \rightarrow \frac{\text{Res}\left\{\frac{e^{iuz} \mathcal{F}_\gamma(z)}{\rho - \mathbf{c}(1 - \gamma/2 - iz, -\gamma/2 + iz)}; i\gamma/2\right\}}{\text{Res}\{e^{iuz} \mathcal{F}_\gamma(z); i\gamma/2\}} \\ = \frac{1}{\rho - \mathbf{c}(1, -\gamma)}.$$

If  $z^* < \gamma/2$ —the supercritical case—the minimal pole is at  $iz^*$  for  $I_n$  and at  $i\gamma/2$  for  $I_d$ , so

$$P_1/D_1 \rightarrow \frac{\text{Res}\left\{\frac{e^{iuz} \mathcal{F}_\gamma(z)}{\rho - \mathbf{c}(1 - \gamma/2 - iz, -\gamma/2 + iz)}; iz^*\right\}}{\text{Res}\{e^{iuz} \mathcal{F}_\gamma(z); i\gamma/2\}} \\ = e^{u(\gamma/2 - z^*)} \cdot \frac{\text{Res}\left\{\frac{\mathcal{F}_\gamma(z)}{\rho - \mathbf{c}(1 - \gamma/2 - iz, -\gamma/2 + iz)}; iz^*\right\}}{\text{Res}\{\mathcal{F}_\gamma(z); i\gamma/2\}} \\ \rightarrow \infty.$$

To see that the price-consumption ratio,  $P_1/C = s \cdot P_1/D_1$ , remains finite in this limit, we must evaluate  $\lim_{s \rightarrow 0} s \cdot P_1/D_1$ . Since  $s = 1/(1 + e^u) \sim e^{-u}$ , we have, asymptotically,

$$P_1/C \rightarrow e^{u(\gamma/2 - z^* - 1)} \cdot \frac{\text{Res} \left\{ \frac{\mathcal{F}_\gamma(z)}{\rho - \mathbf{c}(1 - \gamma/2 - iz, -\gamma/2 + iz)}; iz^* \right\}}{\text{Res} \{ \mathcal{F}_\gamma(z); i\gamma/2 \}},$$

which tends to zero as  $u \rightarrow \infty$  because  $\gamma/2 - z^* - 1 < 0$ .

(ii) For the riskless rate, we seek the limit of

$$R_f = \frac{\int_{-\infty}^{\infty} \mathcal{F}_\gamma(z) e^{iuz} \cdot [\rho - \mathbf{c}(-\gamma/2 - iz, -\gamma/2 + iz)] dz}{\int_{-\infty}^{\infty} \mathcal{F}_\gamma(z) e^{iuz} dz}.$$

This is much simpler, because the minimal pole is  $i\gamma/2$  for both numerator and denominator. It follows that  $R_f \rightarrow \rho - \mathbf{c}(-\gamma/2 - i(i\gamma/2), -\gamma/2 + i(i\gamma/2)) = \rho - \mathbf{c}(0, -\gamma)$ .

(iii) To calculate expected returns, we need the limiting expected capital gain (the first term on the right-hand side of (6)). This is asymptotically equivalent to

$$\frac{\int_{-\infty}^{\infty} \frac{e^{iuz} \mathcal{F}_\gamma(z) \mathbf{c}(1 - \gamma/2 - iz, \gamma/2 + iz)}{\rho - \mathbf{c}(1 - \gamma/2 - iz, -\gamma/2 + iz)} dz}{\int_{-\infty}^{\infty} \frac{e^{iuz} \mathcal{F}_\gamma(z)}{\rho - \mathbf{c}(1 - \gamma/2 - iz, -\gamma/2 + iz)} dz} \equiv \frac{J_n}{J_d},$$

since the higher-order exponential terms  $e^{-mu}$  for  $m \geq 1$ , which appear in (6), become irrelevant exponentially fast as  $u$  tends to infinity. Again, there are two subcases. In the subcritical case, the minimal pole of each of  $J_n$  and  $J_d$  occurs at  $i\gamma/2$ , so

$$\begin{aligned} \lim_{u \rightarrow \infty} \mathbb{E} dP_1/P_1 &= \frac{\text{Res} \left\{ \frac{e^{iuz} \mathcal{F}_\gamma(z) \mathbf{c}(1 - \gamma/2 - iz, \gamma/2 + iz)}{\rho - \mathbf{c}(1 - \gamma/2 - iz, -\gamma/2 + iz)}; i\gamma/2 \right\}}{\text{Res} \left\{ \frac{e^{iuz} \mathcal{F}_\gamma(z)}{\rho - \mathbf{c}(1 - \gamma/2 - iz, -\gamma/2 + iz)}; i\gamma/2 \right\}} \\ &= \mathbf{c}(1, 0). \end{aligned}$$

In the supercritical case, the minimal pole of each of  $J_n$  and  $J_d$  occurs at  $iz^*$ , so

$$\begin{aligned} \lim_{u \rightarrow \infty} \mathbb{E}dP_1/P_1 &= \frac{\operatorname{Res}\left\{\frac{e^{iuz}\mathcal{F}_\gamma(z)\mathbf{c}(1-\gamma/2-iz, \gamma/2+iz)}{\rho-\mathbf{c}(1-\gamma/2-iz, -\gamma/2+iz)}; iz^*\right\}}{\operatorname{Res}\left\{\frac{e^{iuz}\mathcal{F}_\gamma(z)}{\rho-\mathbf{c}(1-\gamma/2-iz, -\gamma/2+iz)}; iz^*\right\}} \\ &= \mathbf{c}(1-\gamma/2+z^*, \gamma/2-z^*). \end{aligned}$$

Since instantaneous expected returns are the sum of expected capital gains and the dividend-price ratio, expected returns in the asymptotic limit are  $\mathbf{c}(1, 0) + \rho - \mathbf{c}(1, -\gamma)$  in the subcritical case, and  $\mathbf{c}(1 - \gamma/2 + z^*, \gamma/2 - z^*)$  in the supercritical case.

Subtracting the riskless rate, excess returns are  $\mathbf{c}(1, 0) + \mathbf{c}(0, -\gamma) - \mathbf{c}(1, -\gamma)$  in the subcritical case, and  $\mathbf{c}(1 - \gamma/2 + z^*, \gamma/2 - z^*) - \rho + \mathbf{c}(0, -\gamma)$  in the supercritical case. Since  $\rho = \mathbf{c}(1 - \gamma/2 + z^*, -\gamma/2 - z^*)$  by the definition of  $z^*$ , the excess return in the supercritical case can be rewritten as  $\mathbf{c}(1 - \gamma/2 + z^*, \gamma/2 - z^*) + \mathbf{c}(0, -\gamma) - \mathbf{c}(1 - \gamma/2 + z^*, -\gamma/2 - z^*)$ .

*Step 3.* If dividends are also independent across assets, then we can decompose  $\mathbf{c}(\theta_1, \theta_2) = \mathbf{c}_1(\theta_1) + \mathbf{c}_2(\theta_2)$  as described in the text. It follows that, in the subcritical case,  $XS \rightarrow \mathbf{c}(1, 0) + \mathbf{c}(0, -\gamma) - \mathbf{c}(1, -\gamma) = 0$ , and in the supercritical case,

$$\begin{aligned} XS_1 &\rightarrow \mathbf{c}(1 - \gamma/2 + z^*, \gamma/2 - z^*) + \mathbf{c}(0, -\gamma) \\ &\quad - \mathbf{c}(1 - \gamma/2 + z^*, -\gamma/2 - z^*) \\ &= \mathbf{c}_2(\gamma/2 - z^*) + \mathbf{c}_2(-\gamma) - \mathbf{c}_2(-\gamma/2 - z^*). \end{aligned}$$

*Step 4.* This last expression is positive because  $\mathbf{c}_2(x)$ —as a CGF—is convex. To spell things out,  $(\mathbf{c}_2(e) - \mathbf{c}_2(d))/(e - d) < (\mathbf{c}_2(g) - \mathbf{c}_2(f))/(g - f)$  whenever  $d < e < f < g$ . In the supercritical case, we have  $-\gamma < -\gamma/2 - z^* < 0 < \gamma/2 - z^*$ , so  $[\mathbf{c}_2(-\gamma/2 - z^*) - \mathbf{c}_2(-\gamma)]/[(-\gamma/2 - z^*) - (-\gamma)] < [\mathbf{c}_2(\gamma/2 - z^*) - \mathbf{c}_2(0)]/[(\gamma/2 - z^*) - 0]$ , or equivalently, because  $\mathbf{c}_2(0) = 0$ ,  $\mathbf{c}_2(-\gamma/2 - z^*) - \mathbf{c}_2(-\gamma) < \mathbf{c}_2(\gamma/2 - z^*)$ , as required.

*Step 5(i).* Proof that  $R_1 < R_2$ , assuming independence of dividends: In the subcritical case,  $R_1 = \rho + \mathbf{c}(1, 0) - \mathbf{c}(1, -\gamma)$  and  $R_2 = \rho + \mathbf{c}(0, 1) - \mathbf{c}(0, 1 - \gamma)$ . Since we are assuming independence, we must show that  $-\mathbf{c}_2(-\gamma) < \mathbf{c}_2(1) - \mathbf{c}_2(1 - \gamma)$ , or equivalently, that  $\mathbf{c}_2(1 - \gamma) < \mathbf{c}_2(1) + \mathbf{c}_2(-\gamma)$ , which follows by convexity of  $\mathbf{c}_2(\cdot)$ .

In the supercritical case,  $R_1 = \mathbf{c}(1 - \gamma/2 + z^*, \gamma/2 - z^*)$  and  $R_2 = \mathbf{c}(1 - \gamma/2 + z^*, -\gamma/2 - z^*) + \mathbf{c}(0, 1) - \mathbf{c}(0, 1 - \gamma)$  (substituting in for  $\rho$  from the definition of  $z^*$ ). By independence, it remains to show that  $\mathbf{c}_2(\gamma/2 - z^*) < \mathbf{c}_2(-\gamma/2 - z^*) + \mathbf{c}_2(1) - \mathbf{c}_2(1 - \gamma)$ , or equivalently, that  $\mathbf{c}_2(1 - \gamma) + \mathbf{c}_2(\gamma/2 - z^*) < \mathbf{c}_2(1) + \mathbf{c}_2(-\gamma/2 - z^*)$ , which follows by convexity of  $\mathbf{c}_2(\cdot)$ .

*Step 5(ii).* Next, I show that in the supercritical case,  $R_1 \leq G_1$  if  $G_1 \geq G_2$ . We do not need the independence assumption here. Write  $\theta = \gamma/2 - z^* \in (0, 1)$ , so that the limiting  $R_1 = \mathbf{c}(1 - \theta, \theta)$ . The claim is that  $\mathbf{c}(1 - \theta, \theta) \leq \mathbf{c}(1, 0)$ . This follows from the convexity of  $\mathbf{c}(\cdot, \cdot)$ , which implies that  $\mathbf{c}(1 - \theta, \theta) \leq (1 - \theta)\mathbf{c}(1, 0) + \theta\mathbf{c}(0, 1)$ . By assumption,  $\mathbf{c}(0, 1) \leq \mathbf{c}(1, 0)$ , so  $\mathbf{c}(1 - \theta, \theta) \leq (1 - \theta)\mathbf{c}(1, 0) + \theta\mathbf{c}(1, 0) = \mathbf{c}(1, 0)$ , as required.

*Limiting quantities for the large asset.* In the case of the large asset, the assumed finiteness of its price-dividend ratio excludes the possibility that the minimal pole lies below  $(\gamma/2)i$ . If we run through the above logic, the analogue of  $\phi(z)$  is  $\phi_2(z) \equiv \rho - \mathbf{c}(-\gamma/2 + z, 1 - \gamma/2 - z)$ . But now we must have  $\phi_2(\gamma/2) > 0$  by the finiteness condition. So the minimal pole must lie at  $(\gamma/2)i$ , and the result follows by calculating residues there, as above. *Q.E.D.*

**PROOF OF PROPOSITION 7:** We now need to consider the *two* closest residues to the real axis. By assumption,  $z^* \in (\gamma/2 - 1, \gamma/2 + 1)$ , so for price-dividend ratio and excess-return calculations, the closest residue is at  $(\gamma/2)i$  and the next closest is at  $z^*i$ . For the riskless rate calculation, the two closest residues are at  $(\gamma/2)i$  and  $(\gamma/2 + 1)i$ . The residues at  $(\gamma/2)i$  were calculated in the previous section, so it only remains to compute the residues at  $z^*i$  and at  $(\gamma/2 + 1)i$  for the integrands in question. In the case of the dividend yield, we must analyze

$$\begin{aligned} \frac{D_1}{P_1} &= \frac{\int_{-\infty}^{\infty} e^{iuz} \mathcal{F}_\gamma(z) dz}{\int_{-\infty}^{\infty} \frac{e^{iuz} \mathcal{F}_\gamma(z)}{\rho - \mathbf{c}(1 - \gamma/2 - iz, -\gamma/2 + iz)} dz} \\ &\doteq e^{-\gamma u/2} \left/ \left( \frac{e^{-\gamma u/2}}{\rho - \mathbf{c}(1, -\gamma)} \right. \right. \\ &\quad \left. \left. + \frac{\mathcal{B}(\gamma/2 - z^*, \gamma/2 + z^*) e^{-z^* u}}{\mathbf{c}_1(1 - \gamma/2 + z^*, -\gamma/2 - z^*) - \mathbf{c}_2(1 - \gamma/2 + z^*, -\gamma/2 - z^*)} \right) \right., \end{aligned}$$

where the second (approximate) equality follows by the residue theorem logic, as in the previous section,  $\mathcal{B}(x, y) \equiv \Gamma(x)\Gamma(y)/\Gamma(x + y)$ , and  $\mathbf{c}_j(\cdot, \cdot)$  indicates the partial derivative of  $\mathbf{c}(\cdot, \cdot)$  with respect to its  $j$ th argument.

In the subcritical case,  $z^* > \gamma/2$ , straightforward algebra gives

$$\begin{aligned} \frac{D_1}{P_1} &\doteq \rho - \mathbf{c}(1, -\gamma) \\ &\quad + \underbrace{\frac{-\mathcal{B}(\gamma/2 - z^*, \gamma/2 + z^*)[\rho - \mathbf{c}(1, -\gamma)]^2}{\mathbf{c}_1(1 - \gamma/2 + z^*, -\gamma/2 - z^*) - \mathbf{c}_2(1 - \gamma/2 + z^*, -\gamma/2 - z^*)}}_{B_2} \\ &\quad \times e^{-u(z^* - \gamma/2)}, \end{aligned}$$

while in the supercritical case,  $z^* < \gamma/2$ , we have

$$\frac{D_1}{P_1} \equiv \frac{\mathbf{c}_1(1 - \gamma/2 + z^*, -\gamma/2 - z^*) - \mathbf{c}_2(1 - \gamma/2 + z^*, -\gamma/2 - z^*)}{\underbrace{\mathcal{B}(\gamma/2 - z^*, \gamma/2 + z^*)}_{B_4}} \times e^{-u(\gamma/2 - z^*)}.$$

To see that  $B_2 > 0$ , note first that  $\mathcal{B}(\gamma/2 - z^*, \gamma/2 + z^*)$  is negative: it equals  $\Gamma(\gamma/2 - z^*)\Gamma(\gamma/2 + z^*)/\Gamma(\gamma)$ , and  $\Gamma(x)$  is negative for  $x \in (-1, 0)$  and positive for  $x > 0$ . Second, the denominator of  $B_2$  is positive, because it has the opposite sign to the derivative of  $\phi(z) \equiv \rho - \mathbf{c}(1 - \gamma/2 + z, -\gamma/2 - z)$  with respect to  $z$ , evaluated at  $z^*$ . This derivative is negative because  $\phi(z)$  is (i) concave in  $z$ ; (ii) positive at  $z = 0$  by the first finiteness condition in Table I; and (iii) zero at  $z = z^*$  by the definition of  $z^*$ . To see that  $B_4 > 0$ , the same logic shows that the numerator is positive. The denominator is also positive, because  $\gamma/2 - z^* > 0$ , so now  $\mathcal{B}(\gamma/2 - z^*, \gamma/2 + z^*) > 0$ . Similarly,  $B_1 = \gamma[\mathbf{c}(1, -1 - \gamma) - \mathbf{c}(0, -\gamma)]$ ,  $B_3 = B_2[\rho - \mathbf{c}(1, -\gamma)] \cdot Y$ , and  $B_5 = \frac{B_4}{\rho - \mathbf{c}(1, -\gamma)} \cdot Y$ , where

$$Y \equiv [\mathbf{c}(1, 0) - \mathbf{c}(1, -\gamma) + \mathbf{c}(1 - \gamma/2 + z^*, -\gamma/2 - z^*) - \mathbf{c}(1 - \gamma/2 + z^*, \gamma/2 - z^*)].$$

It only remains to show that if the two assets have independent cashflows, then  $Y < 0$  in the supercritical case and  $Y > 0$  in the nearly supercritical case. The former follows as in steps 3 and 4 of the proof of Proposition 6. The latter does too: the inequality is reversed because now  $\gamma/2 < z^*$ . *Q.E.D.*

## APPENDIX B: THE $N$ -TREE CASE

### B.1. *The Expectation*

To make a start, we seek the integral

$$I_N \equiv \int_{\mathbb{R}^{N-1}} \frac{e^{-ix_1z_1 - ix_2z_2 - \dots - ix_{N-1}z_{N-1}}}{(e^{x_1/N} + \dots + e^{x_{N-1}/N} + e^{-(x_1+x_2+\dots+x_{N-1})/N})^\gamma} dx_1 \dots dx_{N-1}.$$

Write  $x_N \equiv -x_1 - \dots - x_{N-1}$  and, for  $j = 1, \dots, N$ , define

$$(37) \quad t_j = \frac{e^{x_j/N}}{e^{x_1/N} + \dots + e^{x_N/N}}.$$

The variables  $t_j$  range between 0 and 1, sum to 1, and satisfy  $e^{x_j} = t_j^N / \prod_{k=1}^N t_k$ . Since  $t_N = 1 - t_1 - \dots - t_{N-1}$ , we can rewrite

$$(38) \quad x_j = N \log t_j - \sum_{k=1}^{N-1} \log t_k - \log \left( 1 - \sum_{k=1}^{N-1} t_k \right), \quad j = 1, \dots, N - 1.$$

To make the change of variables (37), we must calculate the Jacobian  $J \equiv \left| \frac{\partial(x_1, \dots, x_{N-1})}{\partial(t_1, \dots, t_{N-1})} \right|$ . From (38),  $\frac{\partial x_j}{\partial t_k} = \frac{1}{t_N} - \frac{1}{t_k} + \frac{N\delta_{jk}}{t_j}$ , where  $\delta_{jk}$  equals 1 if  $j = k$  and zero otherwise, so

$$\frac{\partial(x_1, \dots, x_{N-1})}{\partial(t_1, \dots, t_{N-1})} = \underbrace{\begin{pmatrix} \frac{N}{t_1} & & & \\ & \frac{N}{t_2} & & \\ & & \ddots & \\ & & & \frac{N}{t_{N-1}} \end{pmatrix}}_{\mathbf{A}} + \underbrace{\begin{pmatrix} 1 \\ 1 \\ \vdots \\ 1 \end{pmatrix}}_{\boldsymbol{\alpha}} \underbrace{\begin{pmatrix} \frac{1}{t_N} - \frac{1}{t_1} \\ \frac{1}{t_N} - \frac{1}{t_2} \\ \vdots \\ \frac{1}{t_N} - \frac{1}{t_{N-1}} \end{pmatrix}'}_{\boldsymbol{\beta}'}$$

To calculate  $J = \det(\mathbf{A} + \boldsymbol{\alpha}\boldsymbol{\beta}')$  we can use the following result.

**FACT 2—Matrix Determinant Lemma:** If  $\mathbf{A}$  is an invertible matrix, and  $\boldsymbol{\alpha}$  and  $\boldsymbol{\beta}$  are column vectors of length equal to the dimension of  $\mathbf{A}$ , then  $\det(\mathbf{A} + \boldsymbol{\alpha}\boldsymbol{\beta}') = (1 + \boldsymbol{\beta}'\mathbf{A}^{-1}\boldsymbol{\alpha}) \det \mathbf{A}$ .

In the present case,  $\det \mathbf{A} = N^{N-1}/(t_1 \cdots t_{N-1})$ , and  $\mathbf{A}^{-1}$  is diagonal with  $t_j/N$  as the  $j$ th entry along the diagonal. It follows that  $J = N^{N-2}/(t_1 \cdots t_N)$ . Writing  $\Pi$  for the product  $\prod_{k=1}^N t_k$  and making the substitution suggested in (37),

$$\begin{aligned} I_N &= \int \frac{\left(\frac{t_1^N}{\Pi}\right)^{-iz_1} \left(\frac{t_2^N}{\Pi}\right)^{-iz_2} \cdots \left(\frac{t_{N-1}^N}{\Pi}\right)^{-iz_{N-1}}}{\left(\frac{t_1 + t_2 + \cdots + t_N}{\Pi^{1/N}}\right)^\gamma} \cdot J dt_1 \cdots dt_{N-1} \\ &= N^{N-2} \int (t_1^{\gamma/N+iz_1+\cdots+iz_{N-1}-Niz_1} t_2^{\gamma/N+iz_1+\cdots+iz_{N-1}-Niz_2} \cdots \\ &\quad \times t_{N-1}^{\gamma/N+iz_1+\cdots+iz_{N-1}-Niz_{N-1}} \cdot t_N^{\gamma/N+iz_1+\cdots+iz_{N-1}}) \frac{dt_1 \cdots dt_{N-1}}{t_1 \cdots t_{N-1} t_N}. \end{aligned}$$

This is a Dirichlet surface integral with range of integration  $[0, 1]^{N-1}$ . As shown in Andrews, Askey, and Roy (1999, p. 34), it can be evaluated in terms of  $\Gamma$ -functions: we have

$$\begin{aligned} I_N &= \frac{N^{N-2}}{\Gamma(\gamma)} \cdot \Gamma(\gamma/N + iz_1 + iz_2 + \cdots + iz_{N-1}) \\ &\quad \cdot \prod_{k=1}^{N-1} \Gamma(\gamma/N + iz_1 + \cdots + iz_{N-1} - Niz_k). \end{aligned}$$

Defining  $\mathcal{G}_\gamma^N(\mathbf{z}) = I_N/(2\pi)^{N-1}$ , where  $\mathbf{z} = (z_1, \dots, z_{N-1})$ , we have

$$(39) \quad \mathcal{G}_\gamma^N(\mathbf{z}) = \frac{N^{N-2}}{(2\pi)^{N-1}} \cdot \frac{\Gamma(\gamma/N + iz_1 + iz_2 + \dots + iz_{N-1})}{\Gamma(\gamma)} \cdot \prod_{k=1}^{N-1} \Gamma(\gamma/N + iz_1 + \dots + iz_{N-1} - N iz_k).$$

Writing  $\mathbf{x} = (x_1, \dots, x_{N-1})$ , it follows from the Fourier inversion theorem that

$$(40) \quad \frac{1}{(e^{x_1/N} + e^{x_2/N} + \dots + e^{-(x_1+x_2+\dots+x_{N-1})/N})^\gamma} = \int_{\mathbb{R}^{N-1}} \mathcal{G}_\gamma^N(\mathbf{z}) e^{iz'\mathbf{x}} d\mathbf{z}.$$

With  $\boldsymbol{\alpha} \equiv (\alpha_1, \dots, \alpha_N)'$  and  $\tilde{\mathbf{y}}_t \equiv (\tilde{y}_{1t}, \dots, \tilde{y}_{Nt})' \equiv (y_{1t} - y_{10}, \dots, y_{Nt} - y_{N0})'$ , we are now in a position to calculate the expectation

$$E = \mathbb{E} \left[ \frac{e^{\boldsymbol{\alpha}'\tilde{\mathbf{y}}_t}}{(e^{y_{10}+\tilde{y}_{1t}} + \dots + e^{y_{N0}+\tilde{y}_{Nt}})^\gamma} \right].$$

Define the  $(N-1) \times N$  matrix  $\mathbf{Q}$  and vectors  $\mathbf{q}_i$  by

$$\mathbf{Q} \equiv \begin{pmatrix} \mathbf{q}'_2 \\ \mathbf{q}'_3 \\ \vdots \\ \mathbf{q}'_N \end{pmatrix} \equiv \begin{pmatrix} -1 & N-1 & -1 & \dots & -1 \\ -1 & -1 & N-1 & \ddots & \vdots \\ \vdots & \vdots & \ddots & \ddots & -1 \\ -1 & -1 & \dots & -1 & N-1 \end{pmatrix},$$

and let  $\mathbf{q}_1 \equiv (N-1, \dots, -1, -1)'$ . Then, with  $\mathbf{Q}(\mathbf{y}_0 + \tilde{\mathbf{y}}_t)$  playing the role of  $\mathbf{x}$  in (40),

$$(41) \quad E = \mathbb{E} \left[ \frac{e^{\boldsymbol{\alpha}'\tilde{\mathbf{y}}_t - \boldsymbol{\gamma}'(\mathbf{y}_0 + \tilde{\mathbf{y}}_t)/N}}{(e^{\mathbf{q}'_1(\mathbf{y}_0 + \tilde{\mathbf{y}}_t)/N} + \dots + e^{\mathbf{q}'_N(\mathbf{y}_0 + \tilde{\mathbf{y}}_t)/N})^\gamma} \right] \\ = e^{-\boldsymbol{\gamma}'\mathbf{y}_0/N} \int \mathcal{G}_\gamma^N(\mathbf{z}) e^{iz'\mathbf{Q}\mathbf{y}_0} e^{c(\boldsymbol{\alpha} - \boldsymbol{\gamma}/N + i\mathbf{Q}'\mathbf{z})t} d\mathbf{z}.$$

### B.2. Prices, Expected Returns, and Interest Rates

Using (41), and writing  $P_\alpha/D_\alpha$  for the price-dividend ratio of an asset paying dividend  $D_{1t}^{\alpha_1} \dots D_{Nt}^{\alpha_N}$ , we have

$$(42) \quad P_\alpha/D_\alpha = C_0^\gamma \int_0^\infty e^{-\rho t} \mathbb{E} \left[ \frac{e^{\alpha_1 \tilde{y}_{1t} + \dots + \alpha_N \tilde{y}_{Nt}}}{(e^{y_{10}+\tilde{y}_{1t}} + \dots + e^{y_{N0}+\tilde{y}_{Nt}})^\gamma} \right] dt \\ = C_0^\gamma \int_{t=0}^\infty e^{-\rho t} \left( e^{-\boldsymbol{\gamma}'\mathbf{y}_0/N} \int \mathcal{G}_\gamma^N(\mathbf{z}) e^{iz'\mathbf{Q}\mathbf{y}_0} e^{c(\boldsymbol{\alpha} - \boldsymbol{\gamma}/N + i\mathbf{Q}'\mathbf{z})t} d\mathbf{z} \right) dt$$

$$\begin{aligned}
&= C_0^\gamma e^{-\gamma' y_0/N} \int \frac{\mathcal{G}_\gamma^N(\mathbf{z}) e^{i\mathbf{z}'\mathbf{Q}y_0}}{\rho - \mathbf{c}(\boldsymbol{\alpha} - \boldsymbol{\gamma}/N + i\mathbf{Q}'\mathbf{z})} d\mathbf{z} \\
&= (e^{\mathbf{q}'_1 y_0/N} + \dots + e^{\mathbf{q}'_N y_0/N})^\gamma \int \frac{\mathcal{G}_\gamma^N(\mathbf{z}) e^{i\mathbf{z}'\mathbf{Q}y_0}}{\rho - \mathbf{c}(\boldsymbol{\alpha} - \boldsymbol{\gamma}/N + i\mathbf{Q}'\mathbf{z})} d\mathbf{z}.
\end{aligned}$$

I assume that  $\text{Re}[\rho - \mathbf{c}(\boldsymbol{\alpha} - \boldsymbol{\gamma}/N + i\mathbf{Q}'\mathbf{z})] > 0$  for all  $\mathbf{z}$ , which (as in the two-asset case) follows from the apparently weaker assumption that  $\rho - \mathbf{c}(\boldsymbol{\alpha} - \boldsymbol{\gamma}/N) > 0$ .

To calculate expected capital gains, use the multinomial theorem in (42) to write the price as

$$P_\alpha = \sum_{\mathbf{m}} \binom{\gamma}{\mathbf{m}} \int \frac{\mathcal{G}_\gamma^N(\mathbf{z}) e^{(\boldsymbol{\alpha} - \boldsymbol{\gamma}/N + \mathbf{m} + i\mathbf{Q}'\mathbf{z})' y_0}}{\rho - \mathbf{c}(\boldsymbol{\alpha} - \boldsymbol{\gamma}/N + i\mathbf{Q}'\mathbf{z})} d\mathbf{z}.$$

The sum is taken over all  $\mathbf{m}$  with nonnegative integer entries adding up to  $\gamma$ . Thus

$$\begin{aligned}
\mathbb{E}dP_\alpha &= \sum_{\mathbf{m}} \binom{\gamma}{\mathbf{m}} \\
&\quad \times \int \frac{\mathcal{G}_\gamma^N(\mathbf{z}) e^{(\boldsymbol{\alpha} - \boldsymbol{\gamma}/N + \mathbf{m} + i\mathbf{Q}'\mathbf{z})' y_0} \mathbf{c}(\boldsymbol{\alpha} - \boldsymbol{\gamma}/N + \mathbf{m} + i\mathbf{Q}'\mathbf{z})}{\rho - \mathbf{c}(\boldsymbol{\alpha} - \boldsymbol{\gamma}/N + i\mathbf{Q}'\mathbf{z})} d\mathbf{z} dt,
\end{aligned}$$

and so, writing  $\Phi_\alpha = (\mathbb{E}dP_\alpha)/(D_\alpha dt)$ , we have

$$\begin{aligned}
\Phi_\alpha &= \sum_{\mathbf{m}} \binom{\gamma}{\mathbf{m}} \int \frac{\mathcal{G}_\gamma^N(\mathbf{z}) e^{(-\boldsymbol{\gamma}/N + \mathbf{m} + i\mathbf{Q}'\mathbf{z})' y_0} \mathbf{c}(\boldsymbol{\alpha} - \boldsymbol{\gamma}/N + \mathbf{m} + i\mathbf{Q}'\mathbf{z})}{\rho - \mathbf{c}(\boldsymbol{\alpha} - \boldsymbol{\gamma}/N + i\mathbf{Q}'\mathbf{z})} d\mathbf{z} \\
&= \sum_{\mathbf{m}} \binom{\gamma}{\mathbf{m}} e^{m_1 \mathbf{q}'_1 y_0/N + \dots + m_N \mathbf{q}'_N y_0/N} \\
&\quad \times \int \frac{\mathcal{G}_\gamma^N(\mathbf{z}) e^{i\mathbf{z}'\mathbf{Q}y_0} \mathbf{c}(\boldsymbol{\alpha} - \boldsymbol{\gamma}/N + \mathbf{m} + i\mathbf{Q}'\mathbf{z})}{\rho - \mathbf{c}(\boldsymbol{\alpha} - \boldsymbol{\gamma}/N + i\mathbf{Q}'\mathbf{z})} d\mathbf{z}.
\end{aligned}$$

The price of a time- $T$  zero-coupon bond is  $B_T = \mathbb{E}e^{-\rho T} (C_T/C_0)^{-\gamma}$ . Using (41),

$$\begin{aligned}
B_T &= e^{-\rho T} C_0^\gamma \mathbb{E} \frac{1}{(e^{y_{10} + \tilde{y}_{1T}} + \dots + e^{y_{N0} + \tilde{y}_{NT}})^\gamma} \\
&= e^{-\rho T} (e^{\mathbf{q}'_1 y_0/N} + \dots + e^{\mathbf{q}'_N y_0/N})^\gamma \int \mathcal{G}_\gamma^N(\mathbf{z}) e^{i\mathbf{z}'\mathbf{Q}y_0} e^{\mathbf{c}(-\boldsymbol{\gamma}/N + i\mathbf{Q}'\mathbf{z})T} d\mathbf{z},
\end{aligned}$$

so the yield (from which the riskless rate follows by l'Hôpital's rule) is

$$\mathcal{Y}(T) = \rho - \frac{1}{T} \log \left\{ \left( e^{q'_1 y_0/N} + \dots + e^{q'_N y_0/N} \right)^\gamma \times \int \mathcal{G}_\gamma^N(\mathbf{z}) e^{i\mathbf{z}'\mathbf{Q}y_0} e^{c(-\gamma/N+i\mathbf{Q}'\mathbf{z})T} d\mathbf{z} \right\}.$$

B.3. *A Final Change of Variables*

These expressions can be simplified by a final change of variables. Define  $\widehat{\mathbf{z}} \equiv \mathbf{B}\mathbf{z}$ , where

$$\mathbf{B} \equiv \begin{pmatrix} N-1 & -1 & \dots & -1 \\ -1 & N-1 & \ddots & \vdots \\ \vdots & \ddots & \ddots & -1 \\ -1 & \dots & -1 & N-1 \end{pmatrix},$$

so

$$\mathbf{B}^{-1} = \frac{1}{N} \begin{pmatrix} 2 & 1 & \dots & 1 \\ 1 & 2 & \ddots & \vdots \\ \vdots & \ddots & \ddots & 1 \\ 1 & \dots & 1 & 2 \end{pmatrix}.$$

It follows that  $\widehat{z}_k = Nz_k - z_1 - \dots - z_{N-1}$ , and that  $\widehat{z}_1 + \dots + \widehat{z}_{N-1} = z_1 + \dots + z_{N-1}$ . The Jacobian can be calculated using the matrix determinant lemma (Fact 2 above):  $\det \mathbf{B}^{-1} = 1/N^{N-2}$ , so—since  $\mathbf{z} = \mathbf{B}^{-1}\widehat{\mathbf{z}} - d\mathbf{z}$  is replaced by  $d\widehat{\mathbf{z}}/N^{N-2}$ . Next,  $\widehat{\mathbf{z}}$  was defined in such a way that  $\mathcal{G}_\gamma^N(\mathbf{z})$ , defined in equation (39), is equal to  $N^{N-2}\mathcal{F}_\gamma^N(\widehat{\mathbf{z}})$ , defined in the main text. Finally, noting that  $\mathbf{B}^{-1}\mathbf{Q} = \mathbf{U}$  and  $\mathbf{u} \equiv \mathbf{U}\mathbf{y}_0$ , as defined in (19), we have  $\mathbf{Q}'\mathbf{z} = \mathbf{Q}'\mathbf{B}^{-1}\widehat{\mathbf{z}} = \mathbf{U}'\widehat{\mathbf{z}}$  and  $\mathbf{z}'\mathbf{Q}\mathbf{y}_0 = \widehat{\mathbf{z}}'\mathbf{U}\mathbf{y}_0 = \widehat{\mathbf{z}}'\mathbf{u} = \mathbf{u}'\widehat{\mathbf{z}}$ . Proposition 8 follows after making these substitutions, dropping the hat on  $\widehat{\mathbf{z}}$ , and setting  $\boldsymbol{\alpha} = \mathbf{e}_j$  for asset  $j$ .

REFERENCES

ANDREWS, G. E., R. ASKEY, AND R. ROY (1999): *Special Functions*. Cambridge, U.K.: Cambridge University Press. [88,106]  
 BARRO, R. J. (2006): "Rare Disasters and Asset Markets in the Twentieth Century," *Quarterly Journal of Economics*, 121 (3), 823–866. [73]  
 BREEDEN, D. T. (1979): "An Intertemporal Asset Pricing Model With Stochastic Consumption and Investment Opportunities," *Journal of Financial Economics*, 7, 265–296. [55]  
 CAMPBELL, J. Y. (1991): "A Variance Decomposition for Stock Returns," *Economic Journal*, 101, 157–179. [78]  
 CAMPBELL, J. Y., AND J. MEI (1993): "Where Do Betas Come From? Asset Price Dynamics and the Sources of Systematic Risk," *Review of Financial Studies*, 6 (3), 567–592. [70]

- CAMPBELL, J. Y., AND T. VUOLTEENAHO (2004): "Bad Beta, Good Beta," *American Economic Review*, 94 (5), 1249–1275. [72]
- CAMPBELL, J. Y., C. POLK, AND T. VUOLTEENAHO (2010): "Growth or Glamour? Fundamentals and Systematic Risk in Stock Returns," *Review of Financial Studies*, 23 (1), 305–344. [72]
- CHEN, H., AND S. JOSLIN (2012): "Generalized Transform Analysis of Affine Processes and Applications in Finance," *Review of Financial Studies*, 25 (7), 2225–2256. [86]
- COCHRANE, J. H. (2008): "The Dog That Did Not Bark: A Defense of Return Predictability," *Review of Financial Studies*, 21 (4), 1533–1575. [56,78]
- COCHRANE, J. H., F. A. LONGSTAFF, AND P. SANTA-CLARA (2008): "Two Trees," *Review of Financial Studies*, 21 (1), 347–385. [57,86]
- CONT, R., AND P. TANKOV (2004): *Financial Modelling With Jump Processes*. Boca Raton, FL: Chapman & Hall/CRC. [90]
- DUMAS, B. (1992): "Dynamic Equilibrium and the Real Exchange Rate in a Spatially Separated World," *Review of Financial Studies*, 5 (2), 153–180. [57]
- EPSTEIN, L., AND S. ZIN (1989): "Substitution, Risk Aversion, and the Temporal Behavior of Consumption and Asset Returns: A Theoretical Framework," *Econometrica*, 57, 937–969. [87]
- FORBES, K. J., AND R. RIGOBON (2002): "No Contagion, Only Interdependence: Measuring Stock Market Comovements," *Journal of Finance*, 57 (5), 2223–2261. [70]
- LONGSTAFF, F. A., AND J. WANG (2012): "Asset Pricing and the Credit Market," *Review of Financial Studies* (forthcoming). [86]
- LUCAS, R. E. (1978): "Asset Prices in an Exchange Economy," *Econometrica*, 46 (6), 1429–1445. [55]
- (1987): *Models of Business Cycles*. Oxford, U.K.: Basil Blackwell. [55]
- MARTIN, I. W. R. (2011): "The Forward Premium Puzzle in a Two-Country World," Working Paper 17564, NBER. [86]
- (2012): "On the Valuation of Long-Dated Assets," *Journal of Political Economy*, 120 (2), 346–358. [65]
- (2013a): "Consumption-Based Asset Pricing With Higher Cumulants," *Review of Economic Studies* (forthcoming). [57,76]
- (2013b): "Supplement to 'The Lucas Orchard'," *Econometrica Supplemental Material*, 81, [http://www.econometricsociety.org/ecta/Supmat/8446\\_Extensions.pdf](http://www.econometricsociety.org/ecta/Supmat/8446_Extensions.pdf); [http://www.econometricsociety.org/ecta/Supmat/8446\\_data\\_and\\_programs.zip](http://www.econometricsociety.org/ecta/Supmat/8446_data_and_programs.zip). [57,66,72]
- MENZLY, L., T. SANTOS, AND P. VERONESI (2004): "Understanding Predictability," *Journal of Political Economy*, 112 (1), 1–47. [57]
- MERTON, R. C. (1973): "An Intertemporal Capital Asset Pricing Model," *Econometrica*, 41 (5), 867–887. [55]
- PÁSTOR, L., AND P. VERONESI (2003): "Stock Valuation and Learning About Profitability," *Journal of Finance*, 58 (5), 1749–1789. [76]
- (2006): "Was There a Nasdaq Bubble in the Late 1990s?" *Journal of Financial Economics*, 81, 61–100. [76]
- PAVLOVA, A., AND R. RIGOBON (2007): "Asset Prices and Exchange Rates," *Review of Financial Studies*, 20 (4), 1139–1181. [57]
- RIETZ, T. A. (1988): "The Equity Premium: A Solution," *Journal of Monetary Economics*, 22, 117–131. [73]
- SANTOS, T., AND P. VERONESI (2006): "Labor Income and Predictable Stock Returns," *Review of Financial Studies*, 19 (1), 1–44. [57]
- (2010): "Habit Formation, the Cross Section of Stock Returns and the Cash-Flow Risk Puzzle," *Journal of Financial Economics*, 98 (2), 385–413. [84]
- SHILLER, R. J. (1989): "Comovements in Stock Prices and Comovements in Dividends," *Journal of Finance*, 44 (3), 719–729. [70]
- SLATER, L. J. (1966): *Generalized Hypergeometric Functions*. Cambridge, U.K.: Cambridge University Press. [96]

- STEIN, E. M., AND R. SHAKARCHI (2003): *Complex Analysis*. Princeton, NJ: Princeton University Press. [63]
- VUOLTEENAHO, T. (2002): “What Drives Firm-Level Stock Returns?” *Journal of Finance*, 57 (1), 233–264. [78]
- WANG, J. (1996): “The Term Structure of Interest Rates in a Pure Exchange Economy With Heterogeneous Investors,” *Journal of Financial Economics*, 41, 75–110. [86]

*Stanford Graduate School of Business, Stanford University, Stanford, CA 94305, U.S.A.; [ian.martin@stanford.edu](mailto:ian.martin@stanford.edu).*

*Manuscript received February, 2009; final revision received July, 2012.*